# Technical Summary of Harmonic Mitigation Completion Project

For: Western Power Distribution plc

Attention: Jacob Lynch
Western Power Distribution
Herald Way
Pegasus Industrial Estate
East Midlands Airport
Castle Donington
DE74 2TU

| | |
|---|---|
| **Client** | Western Power Distribution plc |
| **Client Reference** | P1082004 |
| **PSC Reference** | JK7942-1 |
| **Revision** | 1 |
| **PSC Group Company** | Power Systems Consultants UK Ltd |
| **Prepared by** | Zia Emin (Technical Director) |
| **Date** | 17th February 2022 |

# Document History

| Revision | Date | Description of changes |
|---|---|---|
| 0 | 04-02-2022 | Draft initial issue for WPD comments |
| 1 | 17-02-2022 | Final issue with WPD comments resolved |

| Revision | Date | Author | Peer Review | Approved |
|---|---|---|---|---|
| 0 | 04-02-2022 | Zia Emin | Geoff Love | Zia Emin |
| 1 | 17-02-2022 | Zia Emin | Geoff Love | Zia Emin |

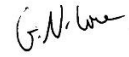

# Executive Summary

This report provides a high-level technical summary of all the work accomplished under the Ofgem funded Network Innovation Allowance entitled Harmonic Mitigation. The main work is undertaken by the University of Swansea for Western Power Distribution with PSC acting as WPD's engineers.

The primary objective of the project was to develop an algorithm that can improve the network's harmonic levels by controlling existing distributed generation inverters. An extended objective was to apply this to multiple inverters as well as testing the performance of the algorithm in a laboratory environment.

The project was executed under four Work Packages:

**Work Package 1** – Following a comprehensive literature review, a project model was established and validated in MATLAB/Simulink environment. This provided a realistic representation of the actual network for the purpose of developing and testing harmonic mitigation algorithms to be overlaid on already included PV inverter models.

**Work Package 2** – A control algorithm was developed to compensate harmonics measured on a feeder considering all the specified requirements. The algorithm includes an adaptive compensation via an automatic gain functionality. The algorithm was proved to be successful in reducing the level of harmonic distortion under varying levels of active power generations and with changing system harmonic levels and without any adverse effect on the network.

**Work Package 3** – The control algorithm developed was implemented at multiple inverters within the network under study. Optimisation on the operation of the inverters as active filter was carried out by testing multiple feedback points such that the most effective and coordinated mitigation is employed. Additional control functionalities were introduced to limit for example the losses on the inverter transformer.

**Work Package 4** – This covered real-time digital simulation tests under laboratory conditions following extensive setup process. The overall simulations indicated a very close agreement between MATLAB/Simulink simulations and the HIL test output.

The overall conclusion following the successful results of WP4 is that the control algorithm developed is effective in reducing the harmonic distortion present in distribution networks.

There were key takeaways that could have been anticipated at earlier stages such as the capabilities of the analytical platforms used for the simulations and recording and usage of measured data sampling. Other key learning points related to the control algorithm were overcome during the execution of the project in effect resulting in a more optimised control algorithm design.

Overall, the project should be classified a success story as all objectives have been fulfilled. However, based on the learning points and the observation during the execution of the project, it was possible to identify future work items that will bring more engineering and scientific knowledge to the existing level of understanding.

The key recommendation among all is to work closely with PV farm developers to gather more data on the PV farms, and specifically the collector system and the inverter physical configuration and output filters. This will allow testing the algorithm on models that are closer to the real-time operating conditions.

Finally, further verification tests (such as with multiple inverters) were recommended such that the algorithm is subjected to more realistic network conditions (use of actual instantaneous timeframe instead of condensed time). Following this, the algorithm can be tested in the field by employing limited number of inverters initially during low irradiation period followed by full day testing.

# Contents

# 1. Introduction

Clean energy policies have increased the level of renewable energy sources connecting into electricity supply systems. Integration of renewable energy sources into existing power networks is based on the heavy use of power electronics in the form of inverters (other than hydro generation). Due to the increased use of power electronic devices, it is expected that the level of harmonic distortions in the network will increase, and their management will become a challenge.

## 1.1. Harmonic Distortion in DNO networks

Harmonic distortion is caused by the emission of currents (or voltages) by non-linear devices which then interact with the impedance of the system to create voltage (or current) distortions. Power electronics are one such non-linear device and will emit harmonic currents as part of their normal operation. The harmonic distortion can adversely affect the equipment within the network. Typically, the effect is excessive heating due to increased harmonic currents, which results in premature degradation and eventually catastrophic failure of the effected equipment.

Distribution Network Operators (DNOs) are expecting to see a large number of new connections that use power electronic devices. In a DNO network, there are multiple connection possibilities; for example, solar and wind power parks, residential level rooftop solar generation, localised EV chargers and so on. Existing solutions for managing harmonics may not be suitable for dynamic networks with varying operating conditions or can create significant cost challenges. Therefore, it is becoming increasingly important to find alternative solutions such that harmonic distortion levels in DNO networks can be managed in a cost-effective way.

## 1.2. Management of Harmonic Distortion

Traditional approaches for managing harmonic distortion include installation of passive shunt filters, usually tuned to specific harmonic orders to deal with specific sources of harmonic emission. The passive filters use a combination of inductive, capacitive and resistive elements acts as low impedance path to earth for harmonic currents thereby acting like a sink. However, in cases where increased harmonic levels are a function of operational conditions such solutions can be proven to be economically disadvantageous on the basis that they are used only in a limited capacity whilst they are continuously connected to the network with associated losses.

Active filtering can be a good alternative. An active filter (AF) is effectively another device employing power electronics (i.e., another inverter) that emits harmonic currents in opposite phase angle, thereby cancelling those that are in the network. They can be stand-alone devices or can be implemented as additional control functionality within existing inverters.

## 1.3. Report Purpose

This report provides a high-level technical summary of all the work accomplished and is mainly based on the published report under each work package [1, 2, 3, 4]. The project is funded by Ofgem's Network Innovation Allowance (NIA) fund and was registered with project reference NIA_WPD_043. The main research work is undertaken by the University of Swansea for Western Power Distribution (WPD) with Power Systems Consultants Ltd UK (PSC) acting as WPD's engineers to support the understanding of the research work.

## 1.4. University of Swansea Project Scope and Structure

Given the background and the desire to control and limit the level of harmonic distortion from distributed sources on the network, the objective of University of Swansea was to develop an algorithm that can improve the network's harmonic levels by controlling existing distributed generation

inverters. The algorithm is aimed to be used not only individually on each inverter but also on multiple inverters concurrently followed by testing in a simulated environment in a laboratory (Hardware-in-the-Loop real time digital simulation). An additional scope of the project is to provide recommendations whether a follow up project is advised to trial the approach in the network.

The project is structured under multiple Work Packages (WP) with clearly defined stages:

**Work Package 1** – Starting with a literature review, this WP is aiming to create a network model that can act as a base model during the investigation.

A detailed literature review was the first task that covers approaches already developed in managing harmonics in the network and any algorithms that relate to the proposed approach in the current project.

On modelling side, a detailed network model was to be created and validated in MATLAB/Simulink environment. The base case harmonic studies will also be run within this WP, providing the reference that will be used to assess the algorithms impact on harmonic levels in the subsequent WPs.

**Work Package 2** – This WP objective is to design, develop and implement a control algorithm that can be introduced to manage a single inverter control. The algorithm should be able to control each inverter individually.

**Work Package 3** – The third WP is aiming to revise the developed algorithm under WP2 such that it can control multiple inverters in order to provide a consolidated control approach in managing harmonic distortion levels on the network.

**Work Package 4** – The final WP is aimed at validating the functionality of the control algorithm on an actual inverter in a laboratory environment using Hardware-in-the-Loop (HIL) testing approach. The reference network model and conditions for demonstration is to be based on WP2 set up due to the availability of only one physical inverter.

# 2. Work Package 1

The first work package consisted of two parts:

- Literature Review
- Model Development and Validation

Literature review concentrated on a comprehensive review of importance of harmonic distortion, mechanism of harmonic distortion generation, their effects, mitigation measures including passive and active filters and their comparative benefits.

The second part consisted of the development of the network model to be used during the investigation and its validation.

## 2.1. Literature Review

University of Swansea's literature review, concentrated on the following subjects:

- Importance of Harmonics
- Passive Filters
- Active Filters
- Control of Active Filters

The following is a summary of their review:

### 2.1.1. Importance of Harmonics

In the context of the project, harmonics were defined as additional sinusoidal components embedded within the power frequency waveform that have frequencies that are integer multiples of the fundamental frequency. They are generated by non-linear devices connected to the power network. Typical non-linear devices include power converters with high power ratings (>1000 MW) such as those in HVDC application as well as much smaller (<100 W) schemes such as those used in household appliances.

Mechanism of harmonic distortion can be explained with reference to Figure 1 where a harmonic voltage drop across the system impedance due to load harmonic current, harmonic currents lead to voltage harmonic distortion at the load bus. In this case any other load connected to the same bus will be subject to the given voltage distortion, and they will draw non-sinusoidal current even if their load is purely resistive. This indicates that harmonics can spread very easily within a given network and consequently affect all equipment connected to the grid.

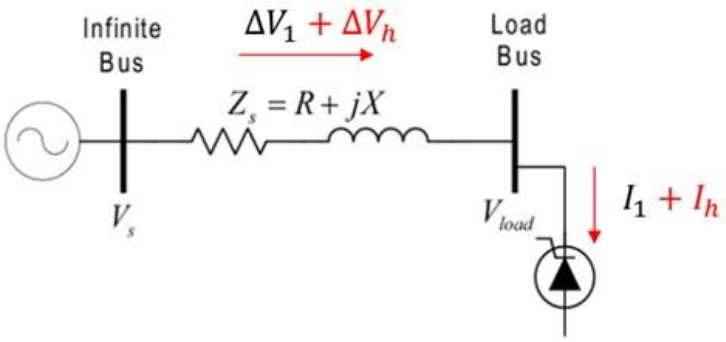


*Figure 1 Mechanism of harmonic distortion*

Increased harmonic distortion result in the following adverse effects:

- Deterioration of power factor correction capacitor banks due to overloading.

- Additional losses in electrical machines, transformers and conductors. On the short term, this causes a reduced efficiency. In the long term, it may lead to reduction of equipment lifetime.
- Errors in measurements when standard instrumentation is used.
- Telephone interference.
- Tripping of protective devices.
- Failure of equipment.

Therefore, to protect the integrity of the assets connected within a power network, it is necessary to develop some form of coordination, and this is achieved by introducing an electromagnetic compatibility concept where different levels of planning, compatibility and immunity are defined. This is supplemented with emission limits issued to individual non-linear connections to minimise propagation of harmonics within the grid. The concept of the emission/planning/compatibility and immunity is illustrated in Figure 2 as indicated in ER G5/5 [5].

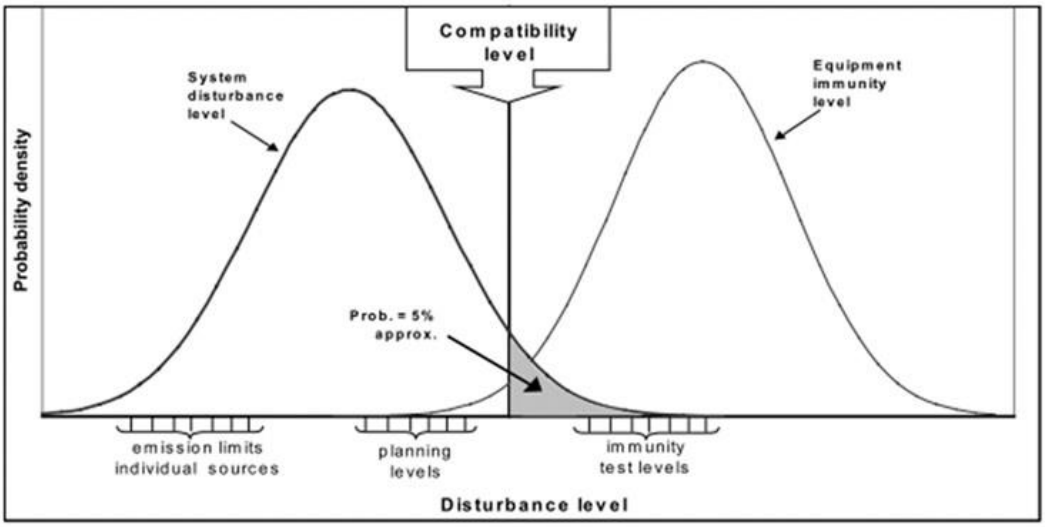


*Figure 2 EMC concept of emission, planning, compatibility and immunity levels [5]*

To maintain a good and acceptable power quality at system level it is important that harmonic levels are controlled. When they are at a level that a breach is likely to take place harmonic mitigating measures are required. The most common approach is the introduction of harmonic filters. A comprehensive overview of available topologies is given in Figure 3.

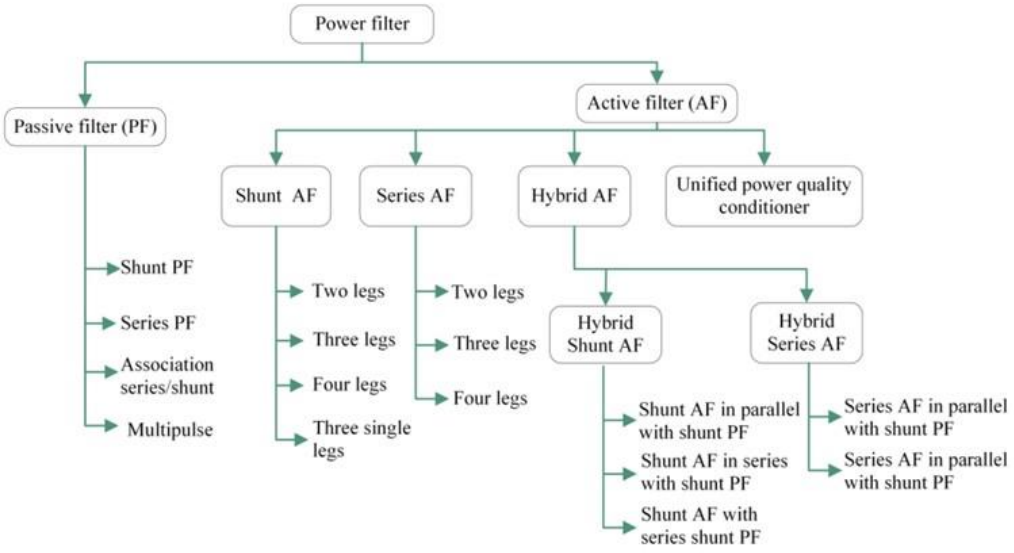


*Figure 3 Various power filter topologies*

## 2.1.2. Passive Filters

Being relatively simple in structure, they have been used extensively and successfully by utilities worldwide to manage harmonics and they are extremely suitable for many applications. They consist of inductances, capacitances, and/or resistors configured and tuned in a way to provide a low-impedance path to ground for harmonic currents. The most common passive filter configurations are:

- Single-tuned filter
- Double-tuned filter
- Damped (or high-pass) filter
- Resonant dumped filter
- Series passive filter

In all cases, the tuning frequency is calculated based on the resonant frequency between an inductor and a capacitor where the overall impedance seen is very low and hence an easy path to earth for harmonic currents. Frequency response of a typical single-tuned passive filter (here tuned to 5$^{th}$ harmonic for illustrative purposes) is shown in Figure 4.

There are some drawbacks and limitations in the use of passive filters. One major issue is related to detuning and this manifests itself as a performance issue associated with deviation from the nominal tuning frequency where reduction in filter effectiveness can be observed. This is driven mainly by factors such as variation of system operating frequency, aging of capacitor or inductors, effect of ambient temperature and tolerances of components.

Other disadvantages of passive filters include the following:

- Good performance only for a limited numbers of harmonics per individual filter.
- Bulky filter components usually due to the need for mitigation being at low orders low order.
- Reduced effectiveness with grid impedance modifications.
- Possible harmonic amplification due to occurrence of new parallel resonances between the grid impedance and the passive filter.

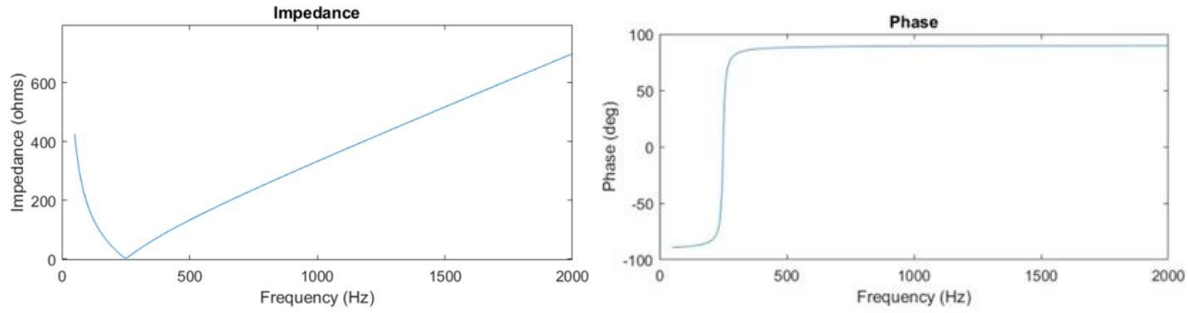


*Figure 4 Frequency response of a single-tuned (tuned to 250Hz) passive filter*

## 2.1.3. Active Filters

The main concept in active filters is the utilisation of power electronics technology to produce specific harmonic components that will cancel those in the network. They are complex with sophisticate control topology and algorithms and can provide other services besides harmonic compensation. There are four different topologies:

**Series active filter:** connected in series with the network through a transformer, injects controllable current to mitigate harmonic voltages. It is placed close to sensitive loads and can control reactive power and voltage sags and swells in addition to harmonics. However, its use is not that commonplace due to high current rating requirements and hence cost prohibited.

**Shunt active filter:** in general, connected in parallel with a non-linear load and injects harmonic currents that are anti-phase to those emitted by the non-linear load and therefore cancellation of harmonic currents at bus level. It is possible to utilise the shunt active filter as reactive power compensation device also thus helping with power factor improvement. They are used very commonly with well-known topologies and a typical example is given in Figure 5. However, implementation at high ratings could be costly.

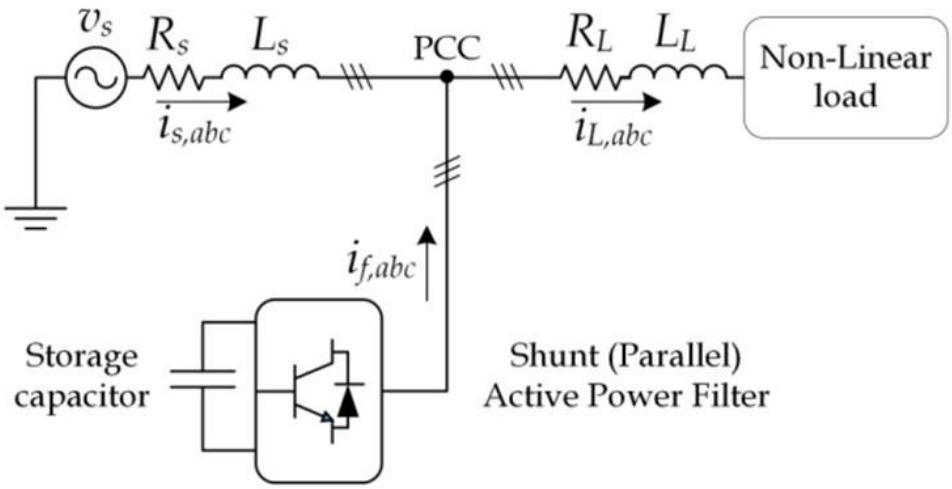


*Figure 5 Typical shunt active filter connection topology*

**Hybrid active filter:** is based on combination of active and passive filters to bring down costs associated with active shunt filters at high ratings. The combination may include variable numbers of active and passive and can help mitigate a broad number of harmonics.

**Unified Power Quality Conditioner (UPQC):** this is a combination of series and shunt active filters and exploits the potential functionality of both topologies without specific tuning requirements of a passive filter. The series part uses a direct voltage controller together with resonant controllers while the shunt part regulates the dc link voltage. It can be used in a versatile way to regulate load voltage, compensate for voltage dips and harmonics, and eliminate load harmonic currents all at the same time. However, the control scheme of a UPQC is very complex and this is the main drawback in their implementation.

Active filter applications are classified based on power ratings. Low power applications are generally employed at residential and commercial buildings with a rating of <100 kvar and generally use high pulse number PWM voltage or current source converters with very fast response time (10 us to 10 ms) and can be single or three-phase. Medium power applications are generally three-phase ranging from 100 kVA to 10 MVA with a response time in the order of tens of milliseconds used primarily at medium to HV distribution systems. High power applications (>10 MVA) tend to be very cost ineffective due to high switching frequency power devices that control the current flow at such levels of power ratings.

## 2.1.4. Control of Active Filters

The basic control scheme of an active filter includes three stages:

- Generation of reference current.
- Current control loop.
- Gate signal generator.

**Generation of reference current:** this first stage involves extracting harmonic components from the distorted current waveform. There are many methods that can be employed either in time-domain or frequency-domain. Typical time-domain approaches include:

- Analogue filters (both high-pass and low-pass)
- Instantaneous reactive power
- Synchronous rotating frame
- Harmonic voltage component detection

Frequency domain approaches include:

- Fast Fourier Transform (FFT)
- Recursive Discrete Fourier Transform (RDFT)
- Wavelet transform
- Dead-beat

In general, the time-domain methods provide a faster response and have a lower computational burden and therefore are more common. The frequency-domain methods have poor transient response, require extensive calculations, and the use of considerable memory

**Current loop control:** this involves identifying and implementing a control strategy that plays the most important role in the performance of the active filter by generating the reference quantities required for the switching signals. The control can operate either with a direct or indirect current measurement as an input. In the case of direct measurement, the load current (and the active filter current but not the source current) is measured directly and fed to the controller, whereas in the case of indirect measurement the source and load currents are measured and fed into the controller. Based on these two measurement approaches utilised, different control strategies can be applied, and these are:

- Control based on instantaneous power
- Control based on instantaneous current
- Control based on synchronous reference frame
- Control based on double synchronous rotating reference frame
- DC-link capacitor voltage regulation

The first is based on calculating the active and reactive power using the direct and quadrature current components from the measured current following transformation from *abc* reference frame into *dq* reference frame. The second method is very similar to the first and effectively ignores the calculation of power but rather uses the instantaneous current in direct and quadrature forms. Transformation into the *dq* reference frame is used in all the other control strategies. Besides these, there are other less commonly employed control strategies such as fuzzy control, artificial neural network, negative sequence current control etc.

Figure 6 shows a typical control strategy based on instantaneous current.

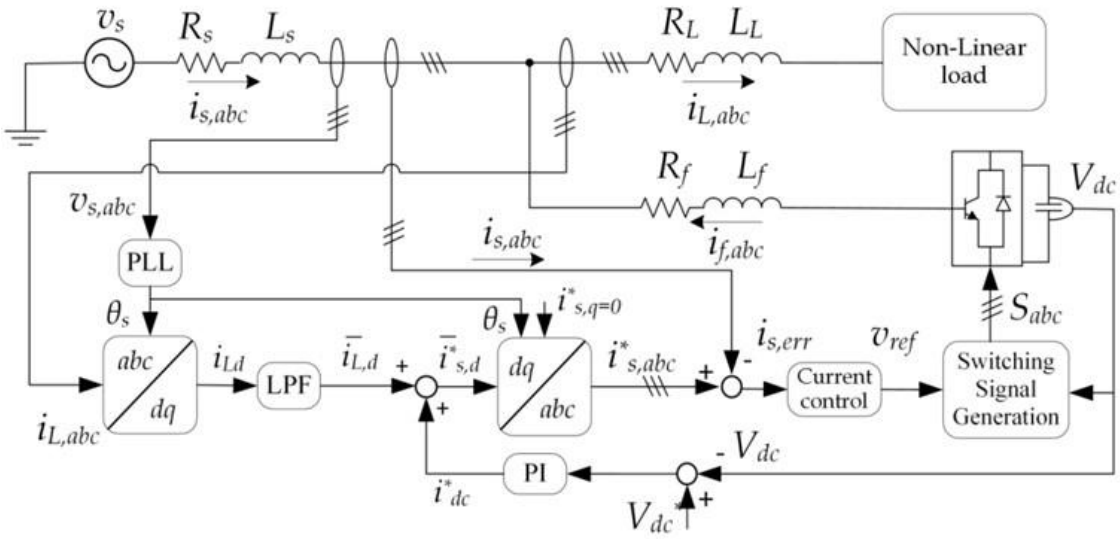


*Figure 6 Instantaneous current control strategy with indirect measurement*

**Gate signal generation:** this last stage involves generation of the gate signal for the converter, and the choice depends on whether it a current or voltage source type converter is employed. A current source converter employs an inductor on the dc-side and it requires a very complex control strategy and hence it is more commonly employed in high power applications where high current carrying capability is a requirement. In a voltage source converter, the dc side includes a capacitor and is more suited for low to medium power applications due to low weight, cost and less complex control strategy. The following list presents the most common techniques used to generate the switching signal for the converter in active filter control:

- Pulse width modulation (PWM)
- Space vector PWM
- Hysteresis control

PWM is one of the most popular signal generation techniques, based on modulating the power converter with a fixed frequency using a carrier signal and shows a typical arrangement of a sinusoidal PWM.

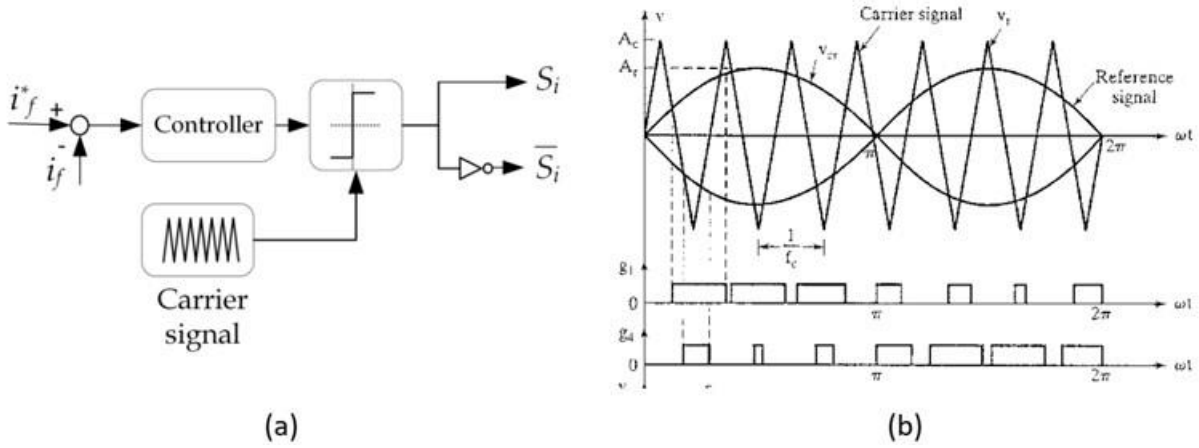


*Figure 7 PWM showing controller and carrier signal (a) and the switching signal generation (b)*

A comprehensive review of examples available from the literature suggests the following summarised points were of importance during the development of the control strategy in the current project:

- Inverter used as active filters in harmonic reduction do not affect the load current
- A control mechanism to derate the harmonic current out of inverter such that the rating is not exceeded is crucial.
- Active filter operation is possible even under fluctuating load current situation since response time is fast.

## 2.2. Model Development and Validation

### 2.2.1. MATLAB/Simulink Model Development

The modelling environment chosen for the project by the University of Swansea was MATLAB/Simulink due to the following reasons:

- Component libraries for electrical power systems modelling and control systems.
- Automated analysis of performance parameters such as harmonics, total harmonic distortion (THD).
- Ability to integrate with real-time OPAL RT-LAB simulation software.

Electrical power network chosen for the study was the Tiverton network as shown in the Single Line Diagram (SLD) Figure 8 supplied by the EXET1 132 kV bus and through two 67.5 MVA grid transformers. The network has five feeders overall and three photovoltaic (PV) farms connected at 33 kV Ayshford (AYSH3), Cullompton (CMPV3) and Stoneshill (STFA3). This network model was provided by WPD in DIgSILENT PowerFactory environment including the wider WPD system beyond EXET1 132 kV node. The model is suitable for harmonic analysis on the basis that it covered recommended modelling in harmonic analysis [6]. The initial task therefore was to create an exact copy of this network in MATLAB/Simulink environment and validate before any further analysis.

An overview of the model created in MATLAB/Simulink is shown in Figure 9. This model includes:

- loads at 11 kV based on SCADA data readings
- 33 kV PV farm model input based on power quality measurements
- an equivalent frequency-dependent 132 kV network impedance (beyond EXET1 node)

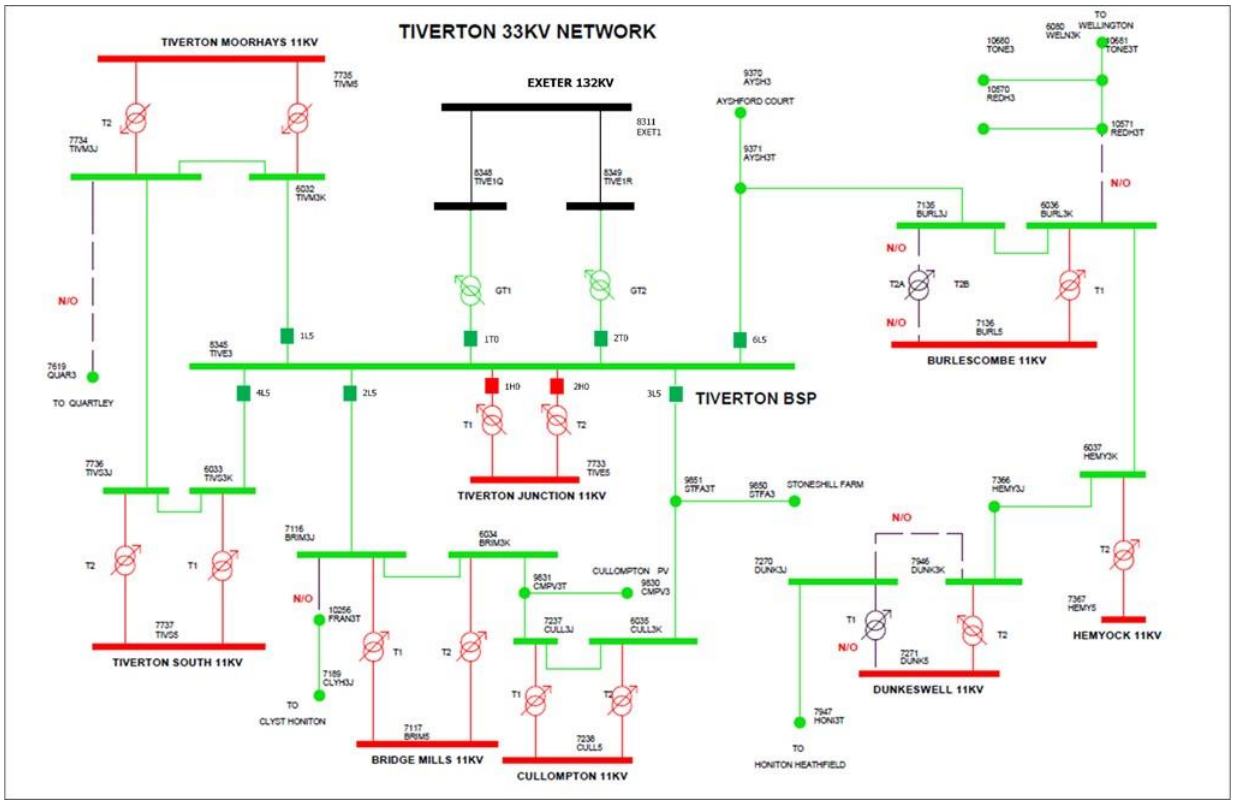


*Figure 8 SLD of the Tiverton Network - for clarity, only the circuit breakers connected to Tiverton BSP are shown*

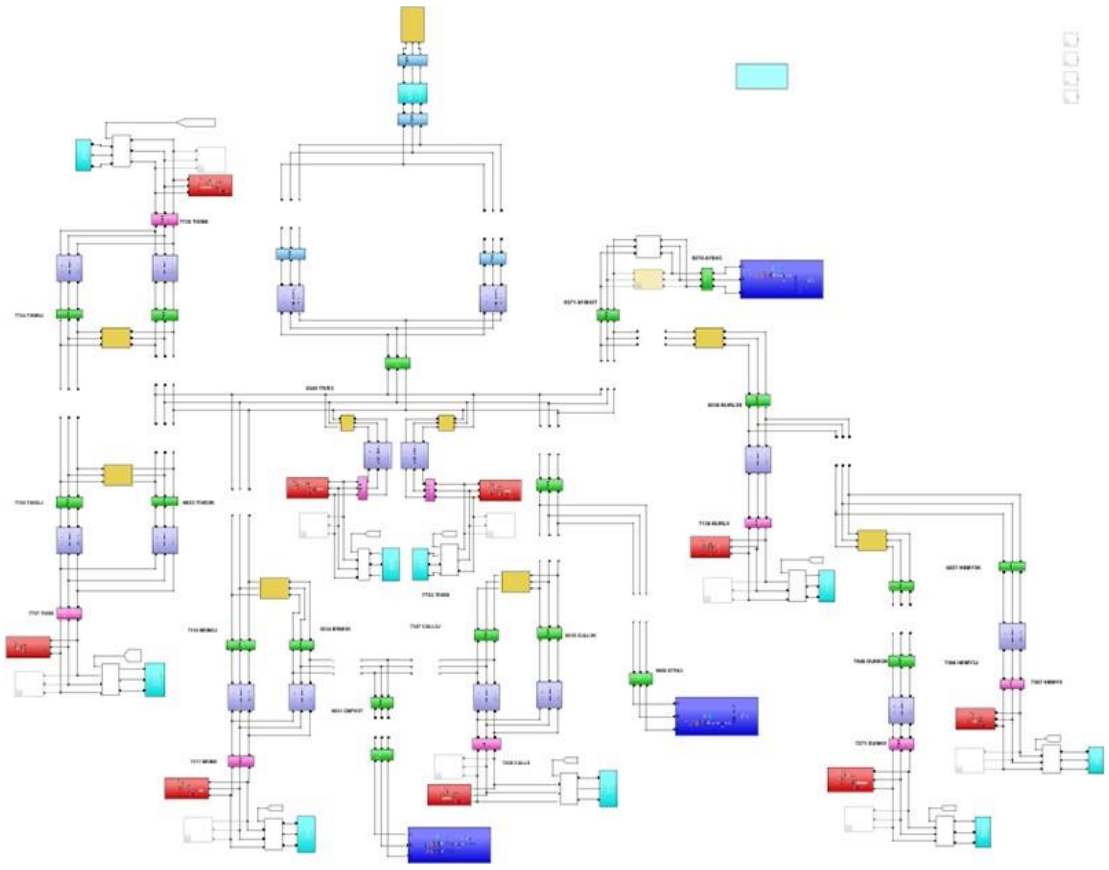

*Figure 9 Overview of the MATLAB/Simulink model*

## 2.2.2. MATLAB/Simulink Model Validation

The model developed in MATLAB/Simulink was validated against the steady-state model in PowerFactory using power flow analysis to check flows on branches and voltage profile on buses as well as a frequency sweep at TIVE3 node.

### 2.2.2.1. Steady-State Power Flow Validation

The following snapshot cases from the available SCADA recording were used for the validation of branch flows and bus voltage profiles:

- Case 1: Winter maximum generation and minimum demand (24/02/19, 13:30: P=3.13 MW at EXET1)
- Case 2: Winter minimum generation and maximum demand (31/01/19, 18:00: P= 50.96 MW at EXET1)
- Case 3: Summer maximum generation and minimum demand (25/08/19, 13:30: P=-8.2 MW at EXET1)
- Case 4: Summer minimum generation and maximum demand (12/06/19, 8:30: P=38.72 MW at EXET1)
- Case 5: Contingency scenario 1 (26/06/19, 10:00: P=31.29 MW at EXET1). This contingency scenario was available in the SCADA data with circuit breaker (CB) 2L5 in open state.
- Case 6: Contingency scenario 2 (24/01/19, 18:30: P= 48.74 MW at EXET1). This contingency scenario was built in the simulation environment from the data provided in order to explore the load unbalance that appears to exist between breakers CB 2L5 and CB 3L5. The initial approach was to model the loads based on the given level and time stamp and this is named as Case 6A, followed by opening of CB 3L5 to derive a contingency labelled as Case 6B.

Table 1 shows active and reactive power values at the system boundary for the six cases as calculated by PowerFactory and MATLAB/Simulink and as recorded by SCADA. Comparison of the values indicate very close agreement between the two modelling platforms and that of the SCADA recording.

*Table 1 Comparison of the active and reactive power values at the system boundary (EXET1)*

| Case | DIgSILENT PowerFactory Model | | MATLAB/Simulink Model | | SCADA data | |
|---|---|---|---|---|---|---|
| | P (MW) | Q (Mvar) | P (MW) | Q (Mvar) | P (MW) | Q (Mvar) |
| 1 | 3.06 | 3.45 | 3.07 | 3.48 | 3.13 | 3.79 |
| 2 | 51.16 | 7.77 | 51.19 | 7.95 | 50.96 | 6.96 |
| 3 | -8.27 | 4.68 | -8.22 | 4.69 | -8.21 | 4.02 |
| 4 | 39.00 | 8.95 | 39.08 | 9.53 | 38.72 | 9.27 |
| 5 | 31.68 | 7.81 | 31.79 | 8.30 | 31.29 | 8.43 |
| 6A | 48.57 | 6.20 | 48.92 | 6.48 | 48.74 | 6.92 |
| 6B | 49.12 | 5.69 | 49.15 | 5.84 | N/A | N/A |

Comparison of voltage profiles based on the power flow are shown in Table 2 and Table 3 and results show very good agreement between models with some differences to the SCADA values. This is to be expected due to inaccuracies in model assumption. For example, due to the lack of tap changer model in MATLAB/Simulink, the tap changer in PowerFactory was also not considered whereas in practice tap changer would be operational and the SCAD values would include this.

*Table 2 Comparison of the voltages at the 11 kV busses and at the 33 kV buses (Cases 1-3)*

| Bus | Text Ref | Rated Voltage | Case 1 | | | Case 2 | | | Case 3 | | |
|---|---|---|---|---|---|---|---|---|---|---|---|
| | | | SCD[1] data | DP[2] Model | ML[3] Model | SCD data | DP Model | ML Model | SCD data | DP Model | ML Model |
| 9830 | CMPV3T (PV) | 33 kV | 1.003 | 1.014 | 1.014 | 0.964 | 0.985 | 0.984 | 0.992 | 1.020 | 1.022 |
| 9850 | STFA3 (PV) | 33 kV | 1.006 | 1.016 | 1.016 | 0.976 | 0.992 | 0.991 | 0.992 | 1.021 | 1.021 |
| 9370 | AYSH3 (PV) | 33 kV | 1.013 | 1.020 | 1.019 | 0.975 | 0.993 | 0.993 | 0.999 | 1.025 | 1.025 |
| 7136 | BURL5 | 11 kV | 1.005 | 1.020 | 1.019 | 1.007 | 0.983 | 0.983 | 1.001 | 1.026 | 1.027 |
| 7367 | HEMY5 | 11 kV | 0.995 | 1.028 | 1.029 | 0.995 | 1.008 | 1.008 | 1.012 | 1.040 | 1.041 |
| 7271 | DUNK5 | 11 kV | 1.007 | 1.023 | 1.024 | 0.991 | 0.975 | 0.975 | 0.998 | 1.030 | 1.031 |
| 7733 | TIVE5-T1 | 11 kV | 0.999 | 1.016 | 1.016 | 0.995 | 0.985 | 0.985 | 0.998 | 1.021 | 1.022 |
| 7733 | TIVE5-T2 | 11 kV | 0.999 | 1.017 | 1.017 | 0.995 | 0.988 | 0.988 | 0.998 | 1.021 | 1.022 |
| 7735 | TIVM5 | 11 kV | 0.992 | 1.009 | 1.009 | 1.006 | 0.979 | 0.979 | 0.988 | 1.014 | 1.014 |
| 7737 | TIVS5 | 11 kV | 1.004 | 1.008 | 1.008 | 1.001 | 0.980 | 0.979 | 0.996 | 1.011 | 1.011 |
| 7117 | BRIM5 | 11 kV | 1.001 | 1.004 | 1.004 | 0.986 | 0.974 | 0.974 | 0.999 | 1.018 | 1.018 |
| 7238 | CULL5 | 11 kV | 1.002 | 1.009 | 1.009 | 0.990 | 0.984 | 0.983 | 0.999 | 1.014 | 1.014 |

[1] SCADA Data
[2] DIgSILENT PowerFactory
[3] MATLAB

*Table 3 Comparison of the voltages at the 11 kV busses and at the 33 kV buses (Cases 4-6)*

| Bus | Text Ref | Voltage | Case 4 | | | Case 5 | | | Case 6A[4] | | | Case 6B | |
|---|---|---|---|---|---|---|---|---|---|---|---|---|---|
| | | | SCD data | DP Model | ML Model | SCD data | DP Model | ML Model | SCD data | DP Model | ML Model | DP Model | ML Model |
| 9830 | CMPV3T(PV) | 33 kV | 0.984 | 0.996 | 0.996 | 0.979 | 0.989 | 0.989 | 0.968 | 0.995 | 0.995 | 0.984 | 0.986 |
| 9850 | STFA3(PV) | 33 kV | 0.993 | 1.001 | 1.001 | 0.990 | 1.000 | 1.000 | 0.979 | 1.001 | 1.001 | 0.993 | 0.996 |
| 9370 | AYSH3(PV) | 33 kV | 0.988 | 1.000 | 1.000 | 0.992 | 1.002 | 1.002 | 0.978 | 0.995 | 0.994 | 0.988 | 0.990 |
| 7136 | BURL5 | 11 kV | 1.001 | 0.998 | 0.988 | 0.993 | 0.995 | 0.995 | 0.998 | 0.983 | 0.983 | 1.001 | 1.003 |
| 7367 | HEMY5 | 11 kV | 0.999 | 1.014 | 1.014 | 0.992 | 1.006 | 1.006 | 0.994 | 0.955 | 0.955 | 0.999 | 1.001 |
| 7271 | DUNK5 | 11 kV | 0.987 | 0.988 | 0.988 | 0.996 | 0.992 | 0.992 | 0.990 | 0.974 | 0.974 | 0.987 | 0.988 |
| 7733 | TIVE5-T1 | 11 kV | 0.995 | 0.993 | 0.993 | 0.995 | 0.999 | 0.999 | 0.990 | 0.991 | 0.991 | 0.995 | 0.993 |
| 7733 | TIVE5-T2 | 11 kV | 0.995 | 0.993 | 0.993 | 0.932 | 0.999 | 0.999 | 0.990 | 0.991 | 0.991 | 0.995 | 0.993 |
| 7735 | TIVM5 | 11 kV | 0.990 | 0.990 | 0.990 | 0.989 | 0.994 | 0.994 | 0.998 | 0.997 | 0.997 | 0.990 | 0.990 |
| 7737 | TIVS5 | 11 kV | 0.990 | 0.980 | 0.980 | 0.987 | 0.984 | 0.984 | 0.985 | 0.999 | 0.999 | 0.990 | 0.988 |
| 7117 | BRIM5 | 11 kV | 0.999 | 0.988 | 0.980 | 0.988 | 0.975 | 0.975 | 0.991 | 1.000 | 1.000 | 0.999 | 0.998 |
| 7238 | CULL5 | 11 kV | 0.988 | 0.990 | 0.981 | 0.990 | 0.985 | 0.983 | 1.000 | 0.992 | 0.992 | 0.988 | 0.990 |

[4] Case 6A is the original case obtained from the SCADA data, Case 6B is built in simulation environment only and therefore SCADA data are not available.

### 2.2.2.2. Frequency Sweep Validation

The second steady-state validation was performed via a frequency sweep where the frequency dependent impedance within both platforms is compared. The importance of frequency dependent impedance is due to the fact that the voltage distortion measured and calculated on the system is a function of the emitted voltages and current and the impedance of the network at the point of interest. The frequency dependent impedance is a function of the resistance, inductance and capacitance of individual components in the network and the way they are connected to each other.

Figure 10 and Figure 11 shows frequency sweep impedance amplitude and phase angle for both model platforms up to the 50$^{th}$ harmonic with remarkable agreement.

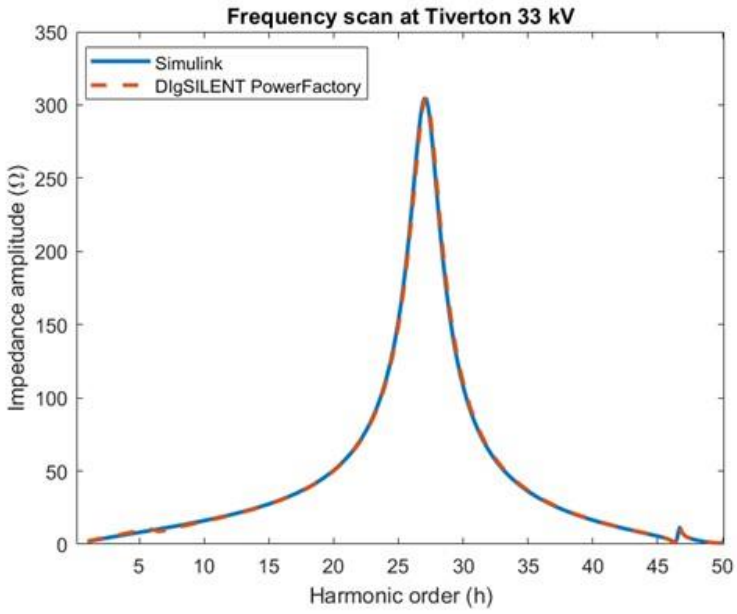


*Figure 10 Amplitude comparison between Simulink and DIgSILENT PowerFactory at TIVE3*

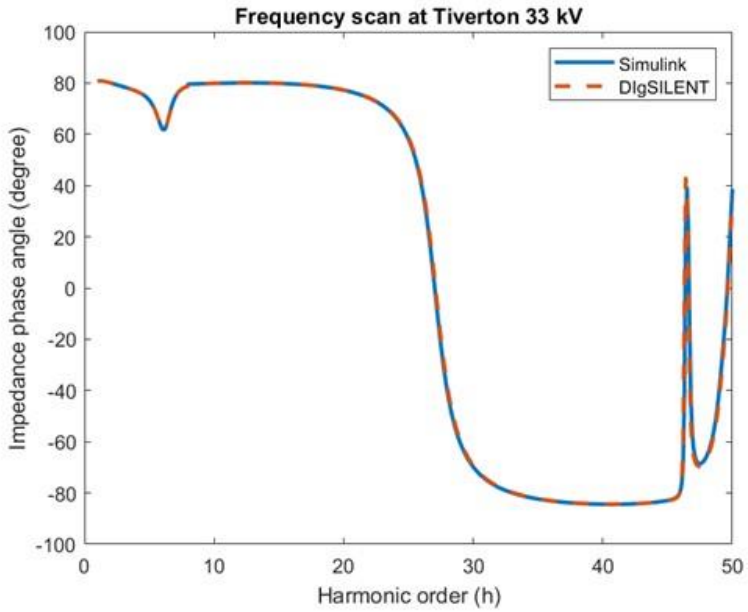


*Figure 11 Phase-angle comparison between Simulink and DIgSILENT PowerFactory at TIVE3*

Based on the steady-state power flow results and the frequency sweep comparison between the two platforms, it was decided that the network topology and component parameters are very similar and therefore the MATLAB/Simulink model can be assumed to be validated model that represents the WPD Tiverton network.

### 2.2.3. MATLAB/Simulink Time-domain Model for EMT Simulations

The next stage in model development was to revise the model such that time-domain EMT simulations that reasonably model fundamental frequency behaviour the actual system can be achieved.

Whilst the same network topology model developed for the power flow analysis is still applicable, dynamic models for both the 11 kV loads and the 33 kV connected PV farms were introduced for the EMT analysis. Load values and PV generation values were derived from the data supplied by WPD. Furthermore, revisions were introduced to the upstream 132 kV equivalent.

The period considered for the EMT analysis was October 2019 with measured power quality data through temporary monitoring equipment. As it is not possible to replicate everything on the second-by-second basis (due to the computational effort required to solve the network in time domain), the simulation time is an acceleration of real time. In this case, 0.1 s of simulation time represents 30 min of real-time and 4.8 s simulation time represents 1 day in real time.

**Dynamic load model (at 11kV busses):** these were represented at all eight 11 kV busses as load time series derived from the half hourly SCADA data. A shunt resistance was added in parallel to dynamic loads creating a stable numerical environment without effecting the results (large value so it acts as open circuit but provides a reference to earth).

In addition to the normal demand part of the load, a dynamic harmonic component was also included, based on a controlled current source. The harmonic part is then able to generate harmonic emissions in accordance with the SCADA active and reactive power but with a scaling factor that is calculated based on power quality measurements such that TIVE3 measured distortion levels can be re-produced.

**PV Farm model:** these were based on a composite model that represents the dynamic behaviour of the PV farm in terms of fundamental power frequency power and harmonic current generation and a detailed inverter model with corresponding control algorithm. The latter was in preparation to the next work package in the project where an active filter was to be added. The inverter model includes a Phase-Lock-Loop (PLL), a dc voltage regulator, a proportional integral (PI) controller and a PWM to generate switching signal. The detailed inverter part modelled for each PV farm is:

- Ayshford: 1 x 500 kVA converter
- Stoneshill: 1 x 800 kVA converter
- Cullompton: 2 x 900 kVA converter

For the remainder of capacity at the PV farms, controlled current sources were modelled that would provide fundamental frequency power as per the power quality measurements. In addition to the power, harmonic current generation capability at $5^{th}$, $7^{th}$, $11^{th}$ and $13^{th}$ harmonics was introduced. The level is based on the power quality measurements as provided.

**Upstream network:** to cater for the harmonic distortion that would penetrate the 33kV network from upstream, an equivalent harmonic voltage connected in series with the frequency dependent network impedance at 132 kV was included. Again, only the four harmonics of interest ($5^{th}$, $7^{th}$, $11^{th}$ and $13^{th}$) were included. The scaling was adjusted such that penetration from upstream accounts for 10% of eth overall distortion at the 33 kV Tiverton bus.

### 2.2.3.1. Fundamental Frequency EMT Model Validation

Digital computers cannot solve continuous-time equations; therefore, they are approximated by a series of solutions at discrete time-steps. For EMT simulations, while the same underlying network topology developed for the power flow analysis was retained, dynamic models for both the 11 kV loads and the 33 kV connected PV farms are introduced as described in the previous sections. In addition, harmonic content of the various components is also included.

The simulation time in EMT analysis domain is an acceleration of real time: in other words, 0.1 s of simulation time represents 30 min of real-time and 4.8 s simulation time represents 1 day in real time. Hence, time plot with seconds in the x-axis should be reviewed considering this accelerated real time. This is done because of the computational effort required to solve the network in time domain.

**Reactive and Active power comparison**

Fundamental frequency power flow validation was performed comparing results with SCADA power flows at the boundary as well as the SCADA voltage profiles to check convergence, stability and validity of the model to represent real system behaviour. Figure 12 shows the SCADA readings for 1st October 2019: between 0 and 0.39 seconds, active and reactive power are equal to zero (the orange markers overlay the blue markers). The SCADA readings are applied at t = 0.4 second so that the model can initialise correctly. The simulation window ends at t = 5.2 s, corresponding to the beginning of data reading for 2nd October 2019.

Figure 13 shows the simulation results illustrating the active and reactive power values used as inputs to the dynamic model. The input values are a linear interpolation of the SCADA readings shown in Figure 12.

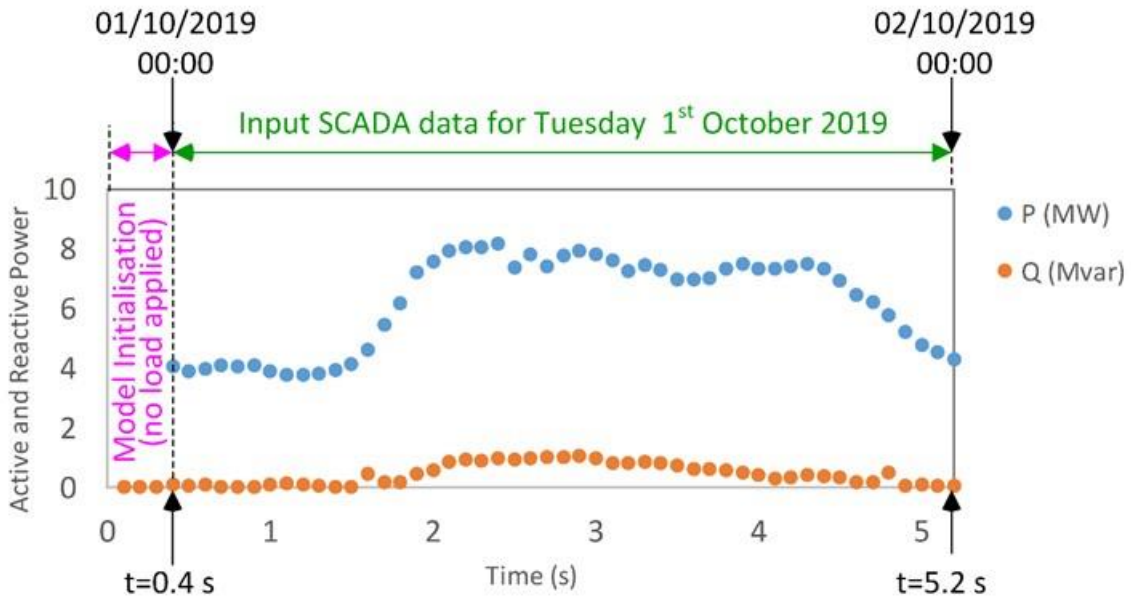


*Figure 12 Active and reactive power SCADA readings for TIVS5*

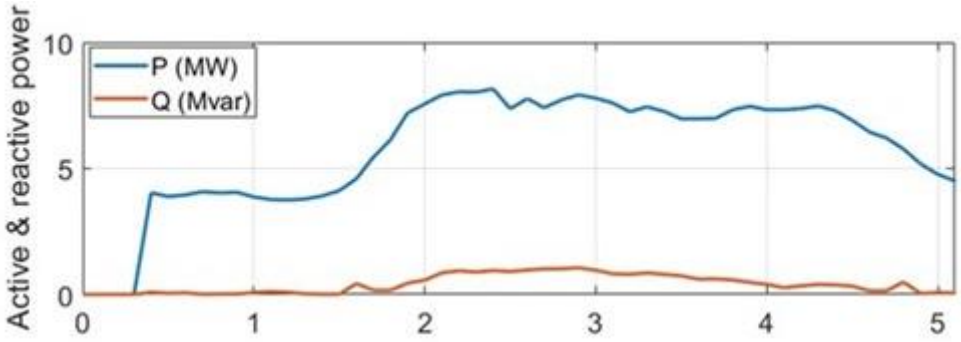


*Figure 13 Simulated active and reactive power for TIVS5*

**RMS voltage comparison**

Figure 14 shows the rms voltage obtained from the simulations and compares it with the rms voltage recorded SCADA data at TIVS5 busbar. The simulation results show oscillations between 2.5 s and 3.5 s that correspond to the rapid fluctuations of PV farm generation. The SCADA data are sampled every 30 minutes and therefore do not show this behaviour. With the increase of the load connected to the system, a voltage drop occurs in the Simulink model. While the SCADA readings show a voltage variation, a similar drop does not occur. This discrepancy is due to the SCADA data including the action of automatic tap-changer transformers to maintain a target voltage during load variation. The transformer blocks used in the Simulink model do not provide the capability for implementing tap changing.

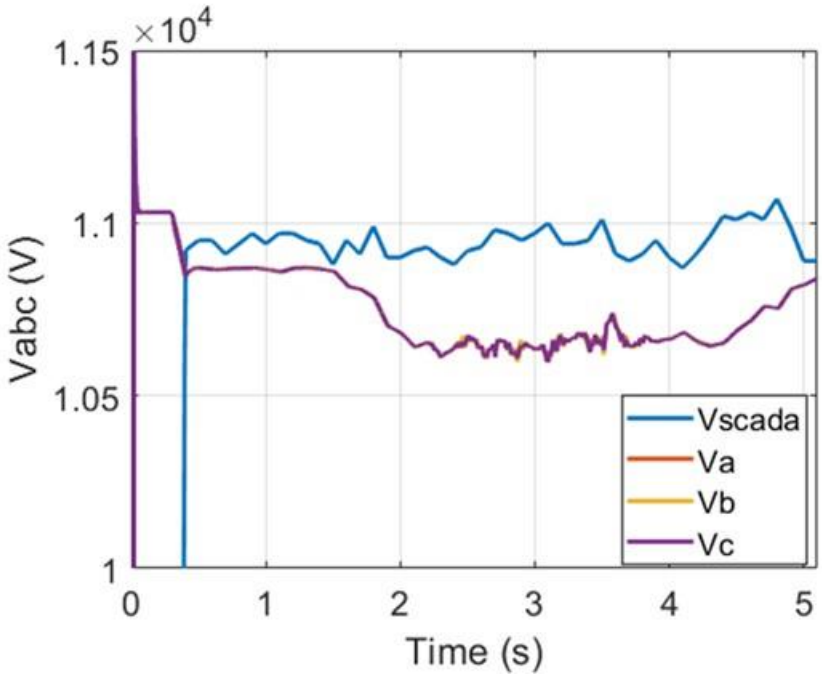


*Figure 14 TIVS5 three-phase rms voltage*

**RMS voltage comparison – including adjusting secondary voltage to take account of the Tap-changer**

Further investigations were carried out at the TIVE3 busbar (i.e. at the bulk supply point) confirming that the observed behaviour is due to the tap changer operation and how this can be taken into account in the simulations. As a result, the transformer ratio at the 132/33 kV transformers (main grid supply transformers) were modified such that the secondary voltage of both 132/33 kV transformers was set to 33.4125 kV to emulate the first tap action bringing the comparison to a much closer alignment as see in Figure 15.

Further instantaneous checks were performed at four different points to confirm that the MATLAB/Simulink EMT model simulation voltages were in line to those calculated by the PowerFactory steady-state model. The checkpoints were chosen to represent points where the system voltage was falling, was rising, was broadly at a lower level, and when the voltage was at a higher level. The voltage rms obtained from the two models are shown in Table 4.

These results showed a good degree of agreement between the voltages calculated by the EMT simulation, and those calculated by power flow analysis within the DIgSILENT PowerFactory model (using P & Q load/generation data taken from the EMT simulation). It was therefore concluded that the MATLAB/Simulink EMT simulation voltages are a reliable indication of the system voltages, and that differences to SCADA are due to the absence of tap changer action in the simulation.

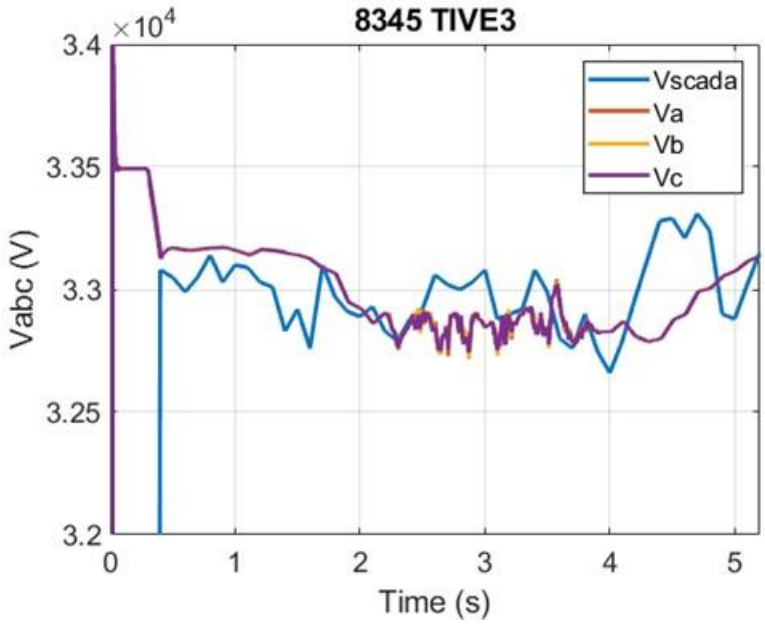


*Figure 15 Comparison of simulation results and SCADA readings for the 33 kV voltage rms at TIVE3 busbar with 132/33.4125 transformer ratio*

*Table 4 Four-point checks to compare voltages generated by MATLAB/Simulink and PowerFactory.*

| Simulation time (s) | TIVE3 voltage pu MATLAB/Simulink EMT | TIVE3 voltage pu PowerFactory Load flow |
|---|---|---|
| 1.5 | 33.20 | 33.23 |
| 2 | 32.90 | 32.98 |
| 4 | 32.87 | 33.12 |
| 4.5 | 32.90 | 32.97 |

**PV farm Active and Reactive power comparison against PQ data and SCADA data**

The performance of the inverters was also validated in terms of fundamental power operation using the composite PV farm model within MATLAB/Simulink. Figure 16 shows the total active power P generated by Ayshford PV farm on 2nd October 2019 along with the power measurement data from the PQ monitor for the same day. The oscillations seen are during the daytime and are due to the solar irradiance variations. A further comparison of the simulated active power at the system boundary is included in Figure 17, and shows a close match to the SCADA data, taking into account the limitations already described above. Results indicate that the power output from the model matches the measured power output confirming the suitability and validity of inverter models for EMT analysis. Comparison of reactive power is not as close as for active power due to some reliability with the

recordings (showing for example zero for several consecutive half-hour periods) but overall a similar pattern between simulated and recorded values can be observed as shown in Figure 18.

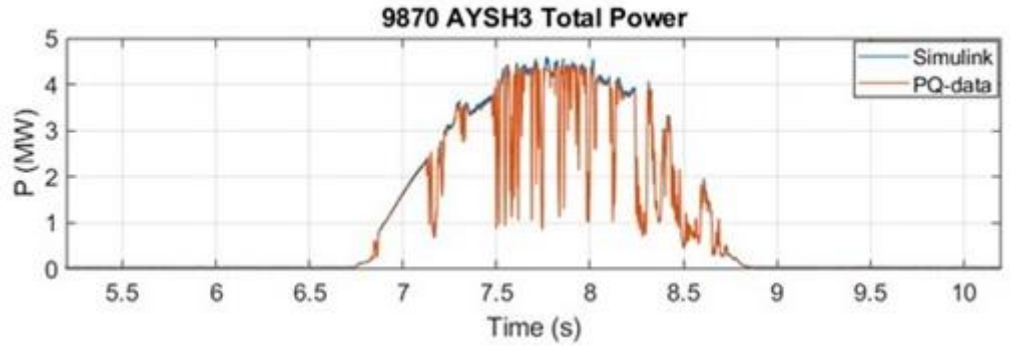


*Figure 16 Power Generated from Ayshford Solar Farm on October 2nd, 2019*

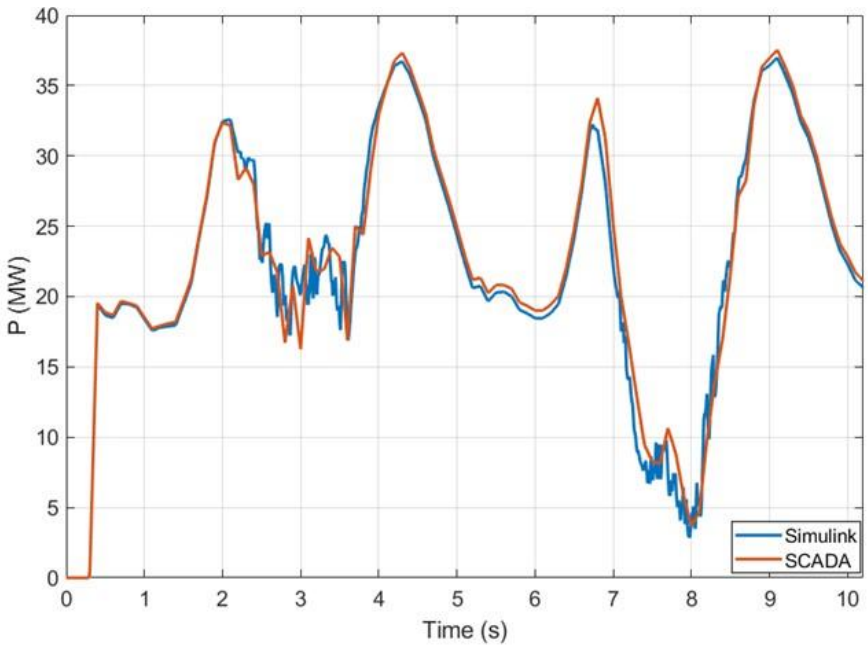


*Figure 17 Total active power at EXET1: comparison between simulation results and SCADA data*

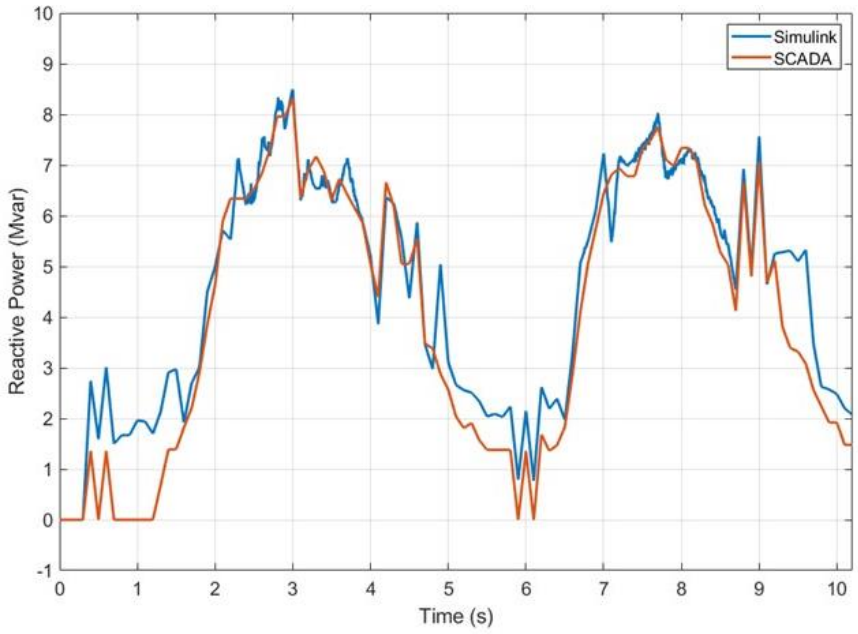


*Figure 18 Total reactive power at EXET1: comparison between simulation results and SCADA data*

### 2.2.3.2. Harmonic Propagation EMT Model Validation

The final validation of the MATLAB/Simulink EMT model is based on the capability to model harmonic propagation behaviour of the network. This was assessed by:

- Comparing modelled current and voltage harmonics to measured PQ data at each of the PV farm sites; and
- Comparing modelled voltage harmonics to PQ monitor data at the BSP 33 kV busbar (TIVE3).

**EMT harmonic validation against measured PQ data at each PV farm site.**

Table 5 show a comparison of measured PQ data with modelled data for current harmonics at the three PV farms. It is noted that he harmonic levels (%) for the four harmonics of interest compare very well to measured values. Whilst the variation of harmonic current level between phases is realistic compared to the actual system measurements, this result was not immediately expected for the simulations, as the model is of a balanced system. This is due to the process of creating the PV sites' generation data model which necessarily involves the modulation of the magnitude of the current waveforms to reflect variation in solar irradiance that introduces small levels of unbalance between the phases. This is accepted as a reasonable artefact of the modelling process observing it as variation in the level of current harmonics between-phases.

In terms of voltage comparison both maximum and minimum voltage harmonics were simulated and compared to measured values as shown in Table 6 and Table 7. It can be seen that the modelled voltage harmonic levels (%) for the four harmonics of interest compare well to measured values, the exception being that the 13$^{th}$ harmonic levels are modelled as slightly higher than the measured levels.

In addition, it was observed that the voltage harmonics were balanced across phases (in all but one instance), as would be expected if the model had balanced load/generation current harmonics and upstream system voltage harmonics. Whilst variations exist between phases for the PV farm site current harmonics the balanced situation observed in voltages is due to the main harmonic contribution coming from the balanced harmonic load modelling and the balanced upstream voltage harmonics distortion. This was checked and confirmed using the Ayshford PV farm alone.

*Table 5 PV farm harmonic currents: comparison of PQ monitoring data and simulation results*

| | PQ monitor data | | | MATLAB model | | |
|---|---|---|---|---|---|---|
| Harmonic order | $I_{12}$ (%) | $I_{23}$ (%) | $I_{31}$ (%) | $I_{12}$ (%) | $I_{23}$ (%) | $I_{31}$ (%) |
| **AYSHFORD** | | | | | | |
| 5 | 1.25 | 1.32 | 1.28 | 1.24 | 1.31 | 1.28 |
| 7 | 0.48 | 0.46 | 0.47 | 0.49 | 0.49 | 0.51 |
| 11 | 0.17 | 0.16 | 0.17 | 0.16 | 0.18 | 0.16 |
| 13 | 0.27 | 0.26 | 0.26 | 0.25 | 0.28 | 0.24 |
| **CULLOMPTON** | | | | | | |
| 5 | 1.04 | 1.17 | 1.10 | 1.07 | 1.20 | 1.03 |
| 7 | 0.48 | 0.43 | 0.45 | 0.45 | 0.47 | 0.43 |
| 11 | 0.10 | 0.10 | 0.10 | 0.09 | 0.11 | 0.08 |
| 13 | 0.05 | 0.05 | 0.07 | 0.06 | 0.08 | 0.06 |
| **STONESHILL** | | | | | | |
| 5 | 0.83 | 0.89 | 0.82 | 0.79 | 0.85 | 0.86 |
| 7 | 0.33 | 0.30 | 0.34 | 0.31 | 0.32 | 0.35 |
| 11 | 0.096 | 0.076 | 0.073 | 0.08 | 0.05 | 0.08 |
| 13 | 0.04 | 0.04 | 0.04 | 0.06 | 0.09 | 0.05 |

*Table 6 Comparison of PV farm maximum harmonic voltages: PQ measurements vs simulation results*

| | PQ monitor data | | | MATLAB model | | |
|---|---|---|---|---|---|---|
| Harmonic order | $V_{12}$ (MAX%) | $V_{23}$ (MAX%) | $V_{31}$ (MAX%) | $V_{12}$ (MAX%) | $V_{23}$ (MAX%) | $V_{31}$ (MAX%) |
| **AYSHFORD** | | | | | | |
| 5 | 1.34 | 1.45 | 1.23 | 1.34 | 1.34 | 1.34 |
| 7 | 1.04 | 1.00 | 1.03 | 1.03 | 1.02 | 1.02 |
| 11 | 0.23 | 0.23 | 0.21 | 0.26 | 0.26 | 0.26 |
| 13 | 0.19 | 0.20 | 0.20 | 0.29 | 0.29 | 0.29 |
| **CULLOMPTON** | | | | | | |
| 5 | 1.49 | 1.58 | 1.41 | 1.44 | 1.44 | 1.44 |
| 7 | 1.04 | 1.00 | 1.14 | 1.15 | 1.15 | 1.15 |
| 11 | 0.23 | 0.24 | 0.27 | 0.28 | 0.28 | 0.28 |
| 13 | 0.18 | 0.25 | 0.28 | 0.31 | 0.31 | 0.31 |
| **STONESHILL** | | | | | | |
| 5 | 1.40 | 1.51 | 1.28 | 1.36 | 1.36 | 1.36 |
| 7 | 1.01 | 1.00 | 1.00 | 1.09 | 1.09 | 1.09 |
| 11 | 0.19 | 0.20 | 0.18 | 0.27 | 0.27 | 0.27 |
| 13 | 0.19 | 0.26 | 0.23 | 0.29 | 0.29 | 0.29 |

*Table 7 Comparison of PV farm minimum harmonic voltages: PQ measurements vs simulation results*

| | PQ monitor data | | | MATLAB model | | |
|---|---|---|---|---|---|---|
| Harmonic order | $V_{12}$ (MIN%) | $V_{23}$ (MIN%) | $V_{31}$ (MIN%) | $V_{12}$ (MIN%) | $V_{23}$ (MIN%) | $V_{31}$ (MIN%) |
| **AYSHFORD** | | | | | | |
| 5 | 0.412 | 0.446 | 0.369 | 0.57 | 0.57 | 0.57 |
| 7 | 0.523 | 0.512 | 0.510 | 0.49 | 0.49 | 0.49 |
| 11 | 0.010 | 0.015 | 0.006 | 0.12 | 0.12 | 0.12 |
| 13 | 0.005 | 0.004 | 0.004 | 0.13 | 0.13 | 0.13 |
| **CULLOMPTON** | | | | | | |
| 5 | 0.565 | 0.614 | 0.537 | 0.61 | 0.61 | 0.61 |
| 7 | 0.553 | 0.555 | 0.553 | 0.56 | 0.56 | 0.56 |
| 11 | 0.003 | 0.024 | 0.004 | 0.13 | 0.13 | 0.13 |
| 13 | 0.004 | 0.003 | 0.004 | 0.19 | 0.19 | 0.19 |
| **STONESHILL** | | | | | | |
| 5 | 0.506 | 0.559 | 0.472 | 0.56 | 0.55 | 0.55 |
| 7 | 0.556 | 0.538 | 0.554 | 0.51 | 0.51 | 0.51 |
| 11 | 0.004 | 0.017 | 0.005 | 0.12 | 0.12 | 0.12 |
| 13 | 0.003 | 0.005 | 0.003 | 0.09 | 0.09 | 0.09 |

**EMT harmonic validation against measured PQ data at BSP 33kV**

The effect of the modelled harmonics at the BSP 33 kV busbar were also assessed. In addition to the four harmonics of interest, the THD values obtained from measurements and simulations at TIVE3 bus were compared for both maximum and minimum harmonic distortion as shown in Table 8 and Table 9. Overall, the simulated harmonic levels compare very well to measured values.

Despite the minor levels of unexpected unbalance observed between phases in the simulation data for PV site current harmonics and the fact that these are accompanied by arguably counter-intuitive balanced voltage harmonics at the PV sites, simulation results compare very well to measured data.

Taking into account the minor discrepancies and the overall results observed, it was concluded that the MATLAB/Simulink EMT simulations provide a realistic model of the harmonic behaviour of the actual network over a three-week time series.

*Table 8 Comparison of maximum harmonic voltages at TIVE3: PQ measurements vs simulation results*

| | PQ monitor data | | | MATLAB model | | |
|---|---|---|---|---|---|---|
| Harmonic order | $V_{12}$ (%) | $V_{23}$ (%) | $V_{31}$ (%) | $V_{12}$ (%) | $V_{23}$ (%) | $V_{31}$ (%) |
| 5 | 1.32 | 1.40 | 1.40 | 1.31 | 1.31 | 1.31 |
| 7 | 1.10 | 1.06 | 1.09 | 1.04 | 1.04 | 1.04 |
| 11 | 0.21 | 0.28 | 0.26 | 0.26 | 0.26 | 0.26 |
| 13 | 0.22 | 0.28 | 0.26 | 0.28 | 0.28 | 0.28 |
| THD | 1.60 | 1.67 | 1.55 | 1.73 | 1.73 | 1.73 |

*Table 9 Comparison of minimum harmonic voltages at TIVE3: PQ measurements vs simulation results*

| | PQ monitor data | | | MATLAB model | | |
|---|---|---|---|---|---|---|
| Harmonic order | $V_{12}$ (%) | $V_{23}$ (%) | $V_{31}$ (%) | $V_{12}$ (%) | $V_{23}$ (%) | $V_{31}$ (%) |
| 5 | 0.470 | 0.513 | 0.412 | 0.52 | 0.52 | 0.52 |
| 7 | 0.52 | 0.521 | 0.511 | 0.49 | 0.49 | 0.49 |
| 11 | 0.004 | 0.019 | 0.005 | 0.12 | 0.12 | 0.12 |
| 13 | 0.003 | 0.004 | 0.003 | 0.10 | 0.10 | 0.10 |
| THD | 0.67 | 0.75 | 0.66 | 0.73 | 0.73 | 0.73 |

## 2.3. Lessons Learned in WP1

Key points that arose during this first stage of the project are centred around the main analysis platform MATLAB/Simulink chosen for this research. The software tool and the input data used for dynamic representation introduced some modelling and operational challenges:

- Lack of tap changer in transformer models could be classified as a major limitation in performing load flow analysis. This was overcome by introducing a representative secondary voltage rather than the nominal level.
- Lack of frequency dependency modelling for most of the power network elements introduced difficulties in accurate harmonic analysis modelling. These were overcome by introducing the information separately into the model.
- Observation of numerical stability issues with the time domain solver. This type of difficulty is seen in other numerical integration algorithms also and is commonly solved by the introduction of a large resistance (which has minimum effect as it acts like an open circuit) such that they have no (or negligible) impact on the simulation results. One peculiar observation was the limitation on connection of multiple current sources to the same node, unless shunt resistors are used.
- Observation of the overall simulation being computationally intensive. This type of difficulty would be seen in other electromagnetic transient analysis environments also with the main driver being the time step and the overall duration of the simulation time. The largest time step that can be used is dictated by the model characteristics and not much can be done about it. The duration of the simulation is split into multiple parts so that simulation time is shortened, and the data generated can be handled easily.
- Input data utilised for models based on SCADA and temporary PQ monitors were observed to be in significantly different time resolution. As the data is an important art of the dynamic models, appropriate scaling had to be applied when the data are imported to ensure that the PV farms and the load models are aligned.

## 2.4. WP1 Concluding Remarks

In addition to the literature review, the key objective of Work Package 1 was to establish and validate an appropriate modelling environment which would be used as base model for the introduction, development and testing of an active filter algorithm to existing solar inverter controllers.

A modelling environment to the key objective has been established in MATLAB/Simulink. Issues associated with the model and its operational implementation have been resolved with the most optimum approach available.

The capability of the developed model has been validated in a time domain study platform for:

- fundamental frequency simulations covering power flow and network bus voltages, and
- harmonic frequencies covering harmonic voltage and current distortions.

Based on the results and analysis undertaken, it has been concluded that the MATLAB/Simulink EMT simulations provide a realistic model of the fundamental and harmonic behaviour of the actual network over a three-week time series.

Overall, it is concluded that the established MATLAB/Simulink modelling environment provides a realistic representation of the actual network for the purpose of developing and testing harmonic mitigation algorithms to be overlaid on already included PV inverter models.

# 3. Work Package 2

The main objective of the second work package was to develop a control algorithm that allows the PV inverter to perform AF operation. This work package focuses on developing this functionality for an individual unit before moving to multiple inverters operating in parallel. In achieving the main objective, the following steps were taken forward and completed by the University of Swansea:

- Specification of control algorithm
- Algorithm design and development
- Testing and validation
- Operational checks.

## 3.1. Specification of Control Algorithm

An important point in designing the control algorithm was to understand that the AF functionality is an added benefit to the PV inverter on top of the main duty of active power generation. With this critical starting item, the following points were to be considered in developing a control algorithm:

- There should be a measured/monitored input that will regulate the level of injection for compensation.
- Any phase shift due to the interface transformer and delays in the acquisition of measurement data will be considered.
- The algorithm would not cause any thermal, voltage, fault level or other constraint in the network.
- The algorithm would not cause the power rating of the inverter to be exceeded.
- Performance of the algorithm would need to be demonstrated via an individual inverter under different operating conditions, including changing inverter output power and changing system harmonic levels.
- The benefits of the algorithm would need to be shown through a detailed comparison of modelled system harmonic performance with and without the harmonic mitigation algorithm.

The individual inverter chosen for the development of the algorithm was Ayshford 0.5 MVA PV inverter connected via a 33/0.4 kV step-up transformer. The arrangement is shown in Figure 19 and due to the load current coming through the radial feeder of Burlescombe, the best measured input to the algorithm was chosen to be the load current on the feeder ($i_{\_load}$ measured at $L_1$) as opposed to points $M_1$ or $F_1$. Current and voltage measured on the high side of the transformer were also used as feedback signals for the control.

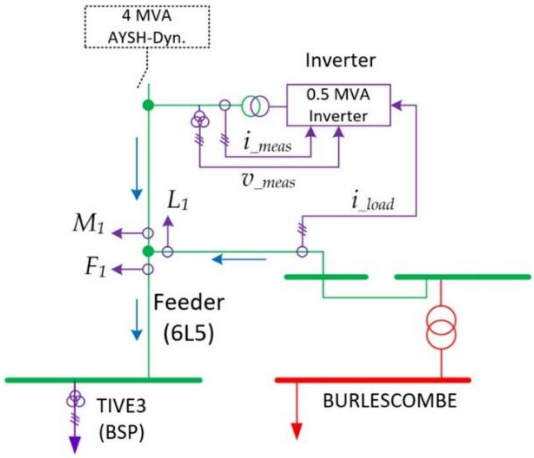


*Figure 19 Arrangement of the Ayshford inverter and the various measurement points (blue arrow indicating direction of normal current flow).*

## 3.2. Algorithm Design and Development

The PV inverter already includes a power controller responsible for the proper active power generation control including some protection functionality. The work therefore involved the design of an additional algorithm that would implement an active filter capability.

There were five key components/stages in the design of the AF control algorithm:

- DC voltage regulation.
- Measurements and *dq* transformation.
- Current Regulation.
- Reference voltage transformation from *dq* frame to *abc* frame.
- Pulse Width Modulation (PWM).

The connectivity of these five key elements is as shown in Figure 20 and the first three are explained in some detail in the next sections. Transformation of the reference voltage from *dq* to *abc* frame is relatively straightforward and the generation of PWM signal is as per the explanation given in section 2.1.4.

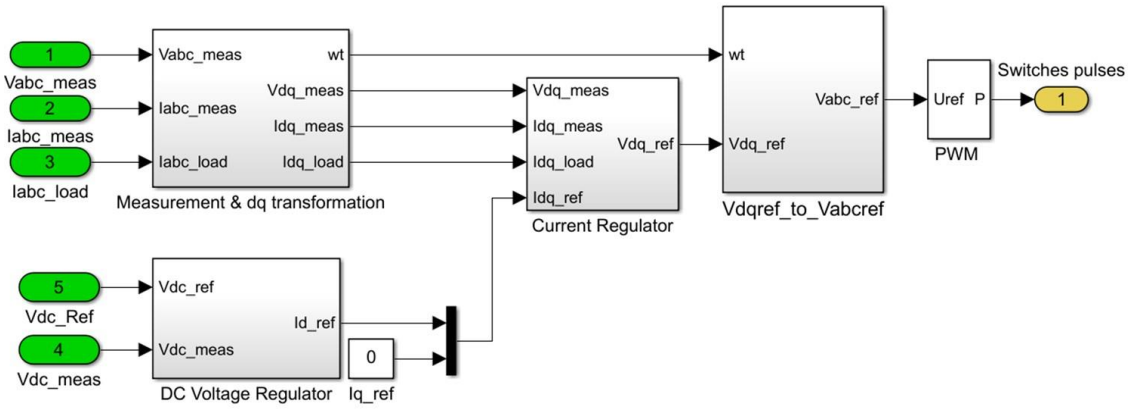


*Figure 20 Key components of the AF control algorithm*

### 3.2.1. DC voltage regulation

This is a key design parameter that controls the calculation of reference current for the inverter at fundamental frequency based on solar irradiance. Addition of AF functionality results in additional harmonic current being superposed to the fundamental and therefore presence of ripple that leads to suboptimal operation. To mitigate this issue the dc voltage reference used was increased from its nominal value of 600 V to 700 V which is still well within the maximum permissible rating.

### 3.2.2. Measurements and *dq* transformation

Three variables are measured for proper operation of the controller: inverter voltage and current, and the load current. Inverter voltage is used in a phase-lock-loop to estimate the grid voltage phase angle and frequency. Transformation from *abc* to the *dq* reference frame is also performed to simplify the control calculations. Harmonic currents within the *dq* frame are seen either in positive or negative sequence components only if they balanced in the *abc* frame. In the case of unbalanced current in *abc* frame, both positive and negative components within the *dq* frame can be seen. For example, for a balanced $5^{th}$ harmonic in *abc* frame (250 Hz), the corresponding *dq* frame will results only in negative sequence component seen at 300 Hz. For an unbalanced $5^{th}$ harmonic in *abc* frame, the corresponding *dq* frame will be a positive component at 200 Hz and a negative component at 300 Hz. A schematic of the measured variables and their transformation from *abc* into *dq* reference frame is shown in Figure 21.

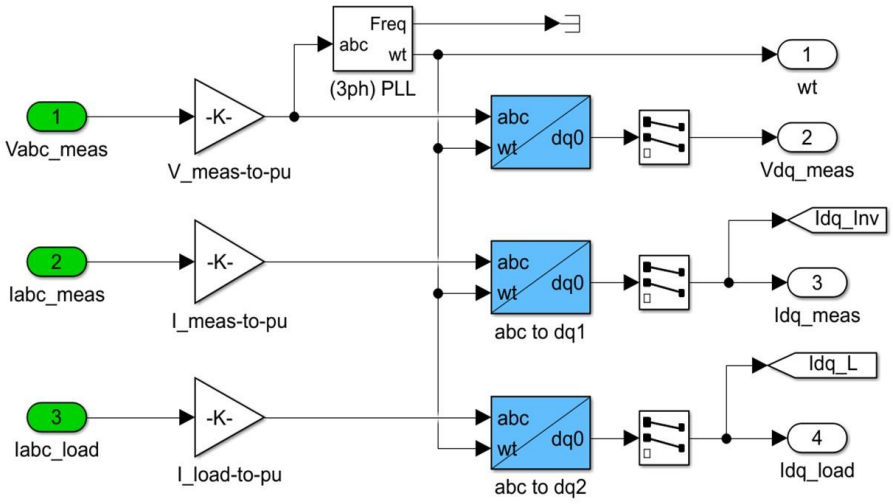


*Figure 21 Schematic of measurements and their transformation from abc to dq reference frame.*

## 3.2.3. Current Regulation

The current regulation itself has three distinct components.

**Harmonic extraction filter:** based on three notch filters they pass specific harmonic frequencies. As the project interest is based on the 5$^{th}$, 7$^{th}$, 11$^{th}$ and 13$^{th}$ order harmonics three notch filters were enough to cover all the components. Unbalance was considered only for the 5$^{th}$ harmonic for testing the validity of the proposed approach when unbalance harmonic components are present. So, a 200 Hz notch filter within the *dq* frame will extract the positive sequence 5$^{th}$, a 300 Hz notch filter will extract the negative sequence 5$^{th}$ and the positive sequence 7$^{th}$, and a 600 Hz notch filter would extract the negative sequence 11$^{th}$ and the positive sequence 13$^{th}$ harmonic. A schematic of the arrangement is shown in Figure 22.

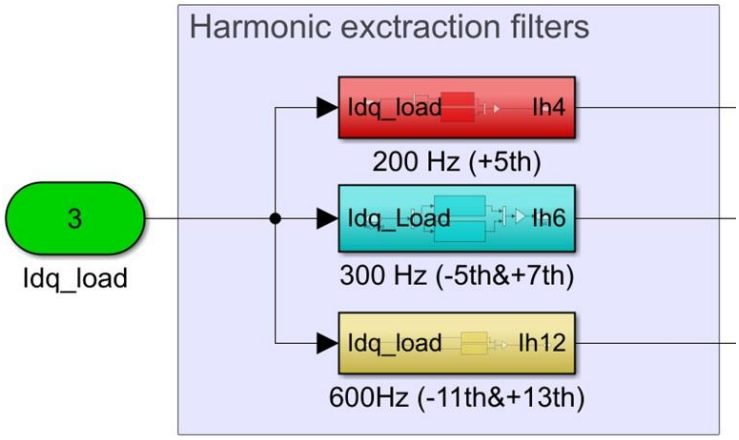


*Figure 22 Harmonic extraction filters in dq reference frame*

**Automatic gain selection:** controls the levels of compensation based on the capacity. The gain value is selected from a look up table considering the level of measured inverter current ($Idq\_meas$) after it passes through a low-pass filter and a rate limiter to reduce the fluctuation in the current signal. Adjustment of the automatic gain over time is limited to 10-minuteto prevent rapid set-point fluctuation. The 10-minute adjustment is based on the most common indices measurement in IEC 61000-4-30. The level of gain changes between 0 and 1 with 1 denoting full compensation. A schematic

is shown in Figure 23. The gain is multiplied with extracted harmonic content to evaluate the level of harmonic injection for mitigation purposes, i.e. the level is set separately for each extracted group.

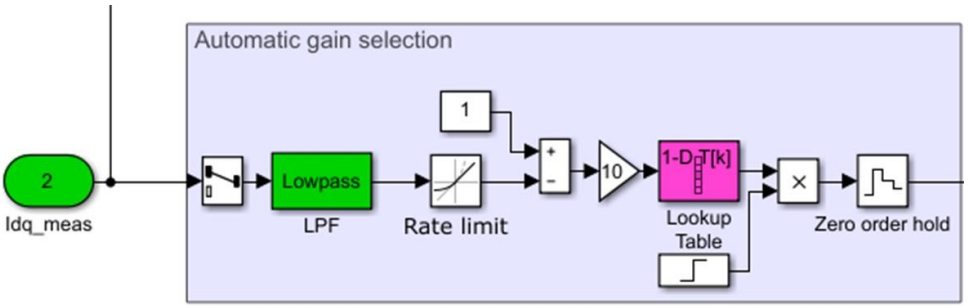


*Figure 23 Schematic of the automatic gain for compensation purposes*

**PI and PR controllers:** while the proportional-integral (PI) controller is used to regulate the fundamental frequency current, three proportional resonant (PR) controllers have been implemented to control each frequency of interest (200, 300 and 600 Hz in *dq* reference frame). The PI and the PR are connected in parallel.

The overall schematic of the current regulation is shown in Figure 24 where the resonant controller and the PI controller connectivity can also be seen along with the reference voltage output which is the main output of the current regulation.

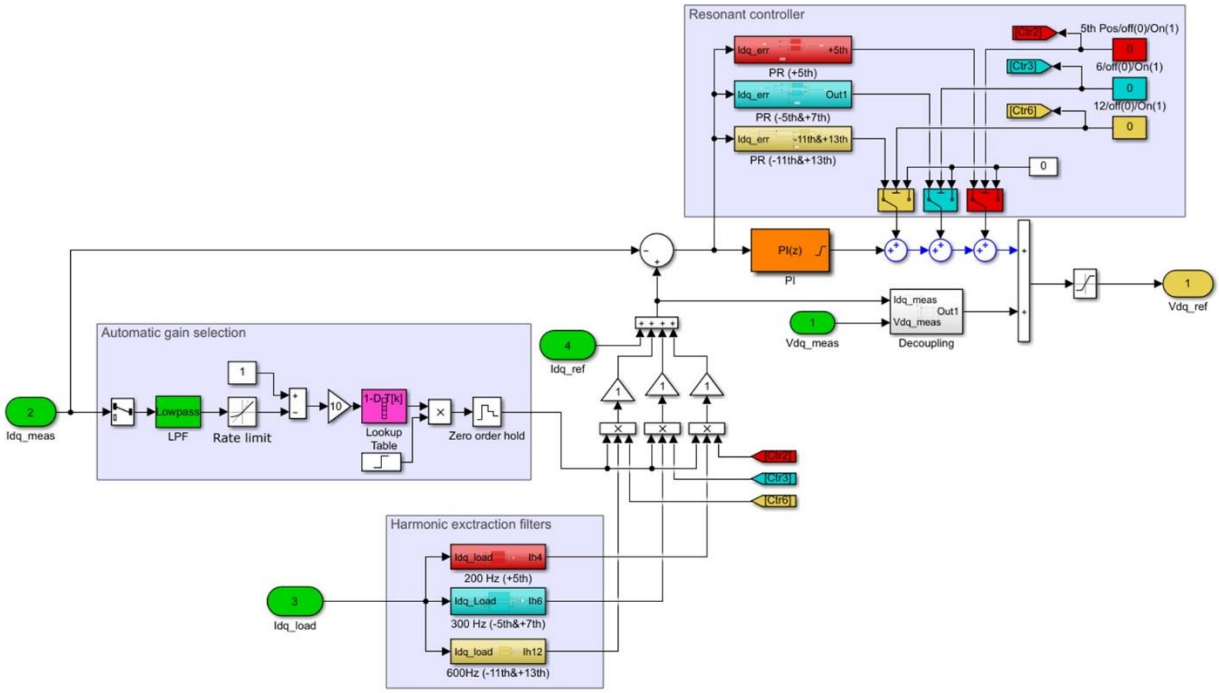


*Figure 24 Schematic of current regulation*

## 3.3. Testing and Validation

With the algorithm completed, some testing was performed in order to validate basic operation of the proposed algorithm.

Tests were performed for individual harmonic on their own, then for each group and eventually for all harmonic components. Due to the nature of transformation into *dq* domain, unbalance $5^{th}$ harmonic currents were introduced to check and validate that the algorithm can operate under unbalance conditions when individual orders do not line up with their classical sequence allocations (for example $5^{th}$ being a negative sequence only harmonic in balanced conditions but having positive and zero sequence content under unbalanced conditions).

During these initial tests, a constant irradiance and harmonic content were assumed. The inverter is assumed to be running at 50% fundamental power output implying that the rest of its capacity is available for compensation purposes.

The following tests were performed:

- Test 1: Balanced $5^{th}$ harmonic current
- Test 2: Unbalanced $5^{th}$ harmonic current (compensating only negative sequence)
- Test 3: Unbalanced $5^{th}$ harmonic current (compensating both positive and negative sequence)
- Test 4: Balanced $7^{th}$ harmonic current
- Test 5: Balanced $5^{th}$ and $7^{th}$ harmonic currents
- Test 6: Balanced $11^{th}$ harmonic current
- Test 7: Balanced $13^{th}$ harmonic current
- Test 8: Balanced $11^{th}$ and $13^{th}$ harmonic currents
- Test 9: Balanced $5^{th}$, $7^{th}$, $11^{th}$ and $13^{th}$ harmonic currents

Figure 25 shows the current waveforms for the load, inverter and feeder currents for Test 9. The presence of the harmonics (in this case all four harmonics of interest) is evident in the load current. The inverter current is a sinusoidal current when generating fundamental power up to the point the compensation is turned on at 0.4 seconds. From then onwards the inverter current is heavily distorted with harmonic that is in anti-phase with the load current. This effect can be clearly seen in the feeder current when at 0.4 seconds the distorted feeder current is cleared of its harmonic content.

Fast Fourier Transformer analysis of the feeder current before and after compensation in Figure 26 proves the point of substantially reduced harmonic content for the $5^{th}$, $7^{th}$, $11^{th}$ and $13^{th}$ harmonic orders. The same outcome has been observed in all the other eight tests that has been performed and the presentation of the output is not repeated here.

Small residual harmonics can be observed (for all the compensated harmonic orders), these represent the limit of the controller action when full compensation is applied. Furthermore, small levels of harmonics are generated at higher order (>1500 Hz) which are due to the result of inverter action. The levels are negligible with no material impact on grid operation.

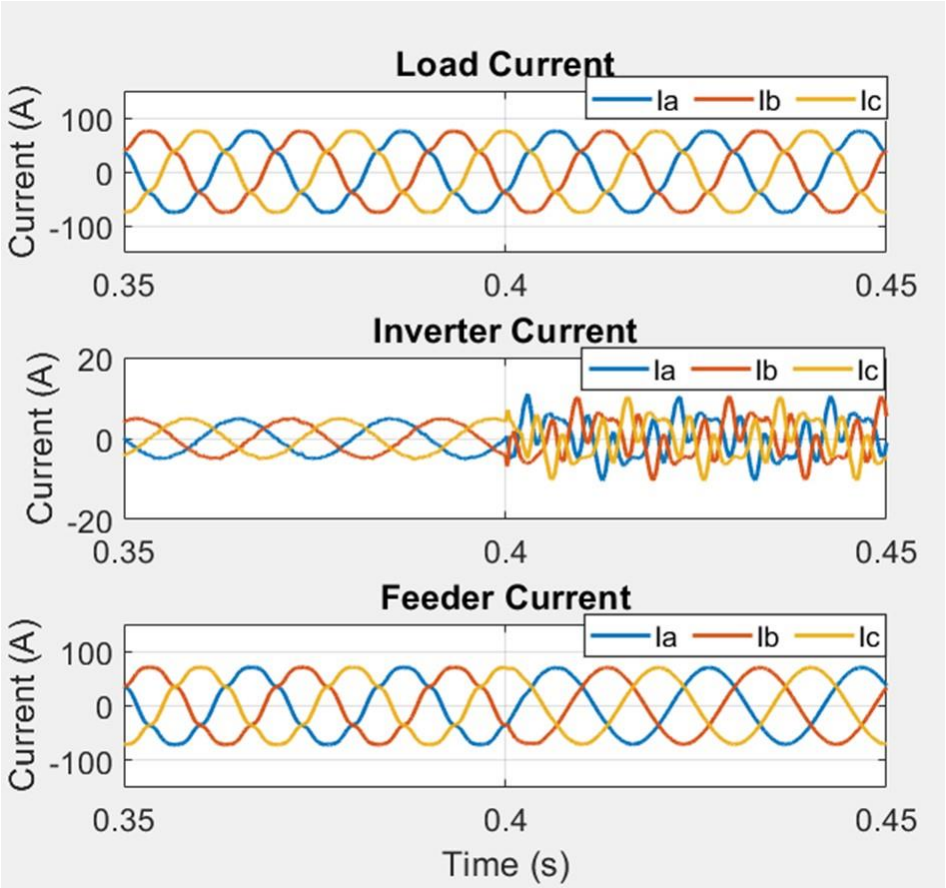


*Figure 25 Current waveforms for load, inverter and feeder before and after compensation for Test 9*

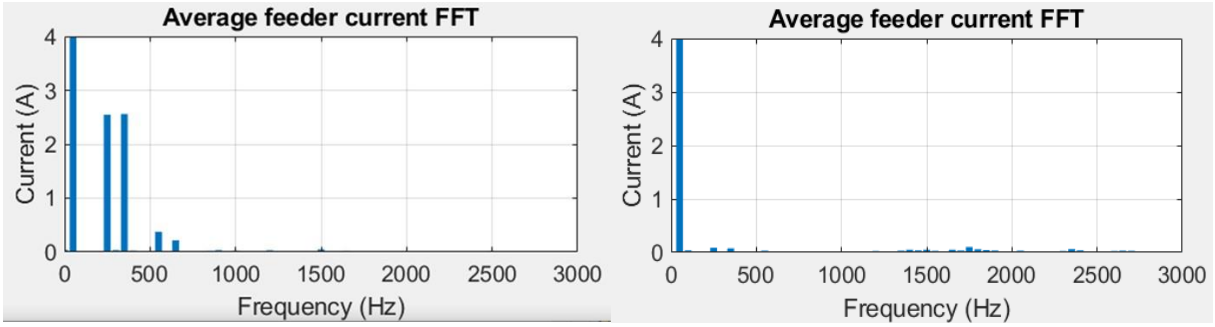


*Figure 26 Fast Fourier Transformer of feeder current before (left) and after (right) compensation*

## 3.4. Operational Studies

Further validation studies were carried out using the Ayshford PV inverter with its additional AF control algorithm. During these operational validation studies, the dynamic model developed and explained in section 2.2.3 was used over a three-week operation. The validation is based on comparing the outcome of harmonic distortion when the network is operating the control algorithm in operation against the network operating without any mitigation.

Four main parameters were monitored and checked in terms of validating the performance of the control algorithm in its effectiveness:

- Inverter current
- Feeder current

- Voltage at bulk supply point
- Transformer losses

## 3.4.1. Inverter Current

The importance of the inverter current is due to the need not to exceed the rated inverter current while performing extra duties in mitigating harmonics. It is desired that the inverter is functioning as an AF during low irradiance times, while at high irradiance it should function on its core duty of producing active power. With reference to Figure 27, the top part shows the inverter current over a period of three weeks while the inverter has no harmonic compensation duty. The burst on data points in the graph corresponds to daytime when irradiance is high or available and the inverter is producing active power. The bottom part of the figure repeats the same simulation but the inverter performing harmonic compensation duty and as it can be seen that the inverter is much more active with harmonic mitigation during low irradiance periods.

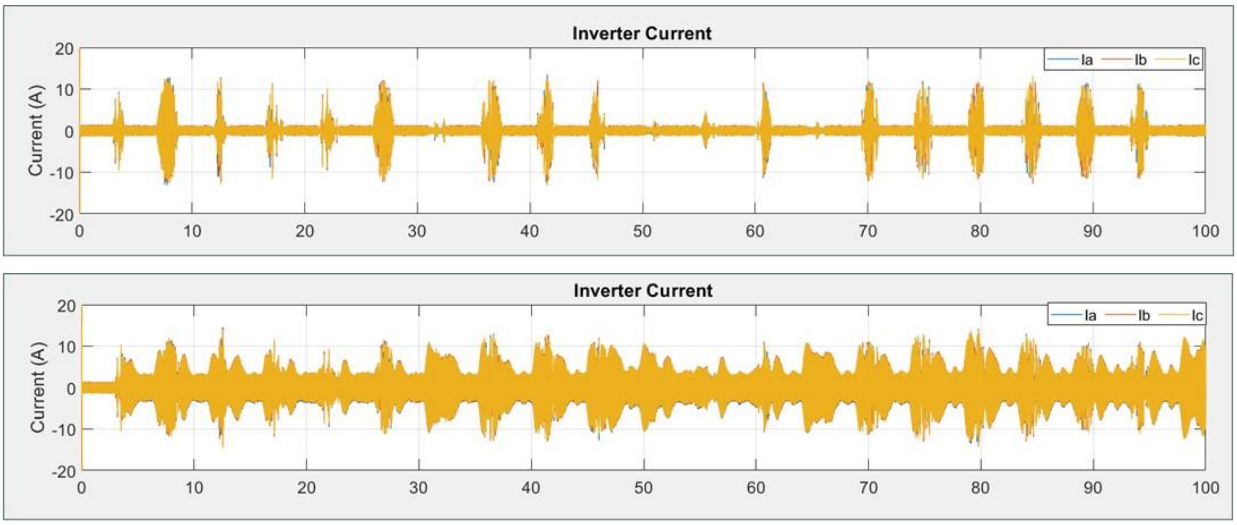


*Figure 27 Inverter current over the entire three-week period with and without compensation (x-axis in seconds with 4.8 s representing 1 day)*

## 3.4.2. Feeder Current

Feeder current was analysed to check the distribution of frequencies in order to establish variation of feeder harmonic current magnitudes with and without harmonic compensation active.

The charts in Figure 28 show the impact of AF operation on 5$^{th}$ harmonic current in the 33 kV feeder over the three-week analysis period. The chart on the left where no compensation is active, shows that the most frequent 5$^{th}$ harmonic current magnitude is around1.3 A, and that currents of up to about 5.8 A can occur, though the number of instances diminishes as the current magnitude increases. The right-hand chart depicts the same analysis with the AF functionality operating, indicating occurrence of significantly different pattern of harmonic currents. The most frequent harmonic current amplitude is around 0.1 A and only very few instances of harmonic current above 0.5 A can be seen which are associated with periods of higher solar irradiance and therefore the inverter does not have sufficient capacity for compensation.

Similar results have been observed for all the other harmonic orders under investigation and the results are not repeated here.

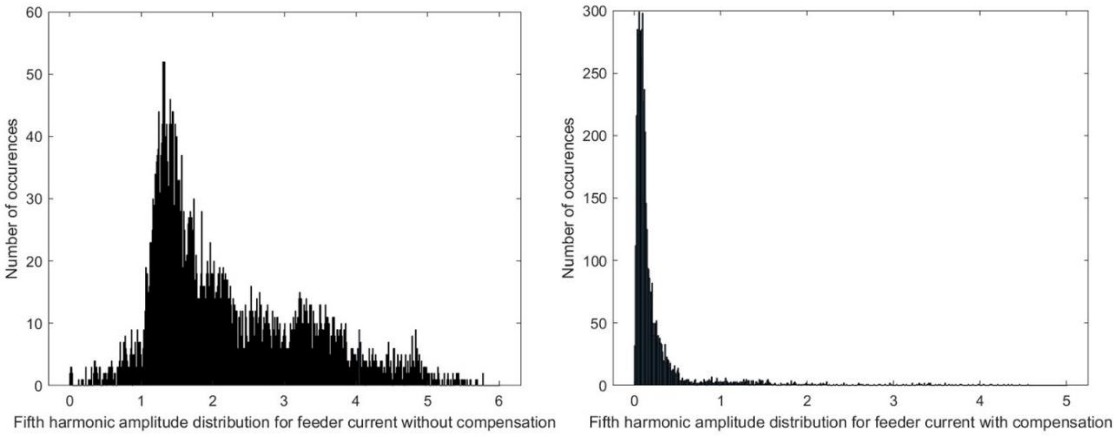


*Figure 28 Frequency distribution for the 5th harmonic amplitude with and without compensation*

Further analysis on the feeder current have been carried out by establishing an average FFT over three-week simulation period. Shows the percentage harmonic content levels with and without compensation and the reduction achieved with the compensation.

*Table 10 Feeder current FFT analysis results*

| Harmonic | Feeder current (A) no compensation | Feeder current (A) with compensation | Percentage reduction (%) |
|---|---|---|---|
| 1st | 57.45 | 57.46 | - |
| 5th | 2.178 | 0.269 | 87.7 |
| 7th | 1.275 | 0.168 | 86.8 |
| 11th | 0.194 | 0.053 | 72.6 |
| 13th | 0.142 | 0.047 | 66.9 |

## 3.4.3. BSP Voltage THD

An important parameter for overall system performance indication is the voltage THD level at Tiverton 33 kV BSP. Calculation of voltage THD for the entire three-week period resulted in an overall reduction of 15.7%, from an initial value of 1.199% to 1.043%. However, higher levels of reduction have been observed for peak level of THD and this shown in the more detailed analysis conducted over a three-day period.

Figure 29 shows the results of voltage THD calculation at TIVE3 bus (BSP) over a three-day period with and without compensation. Detailed comparison has been carried out at the shown peak points all occurring at night-time period. Further comparison on daily average (taking a 7-hour window) and over three days is also performed, and all are detailed in Table 11. The effectiveness of the inverter as an AF during night-time is more pronounced as it is expected.

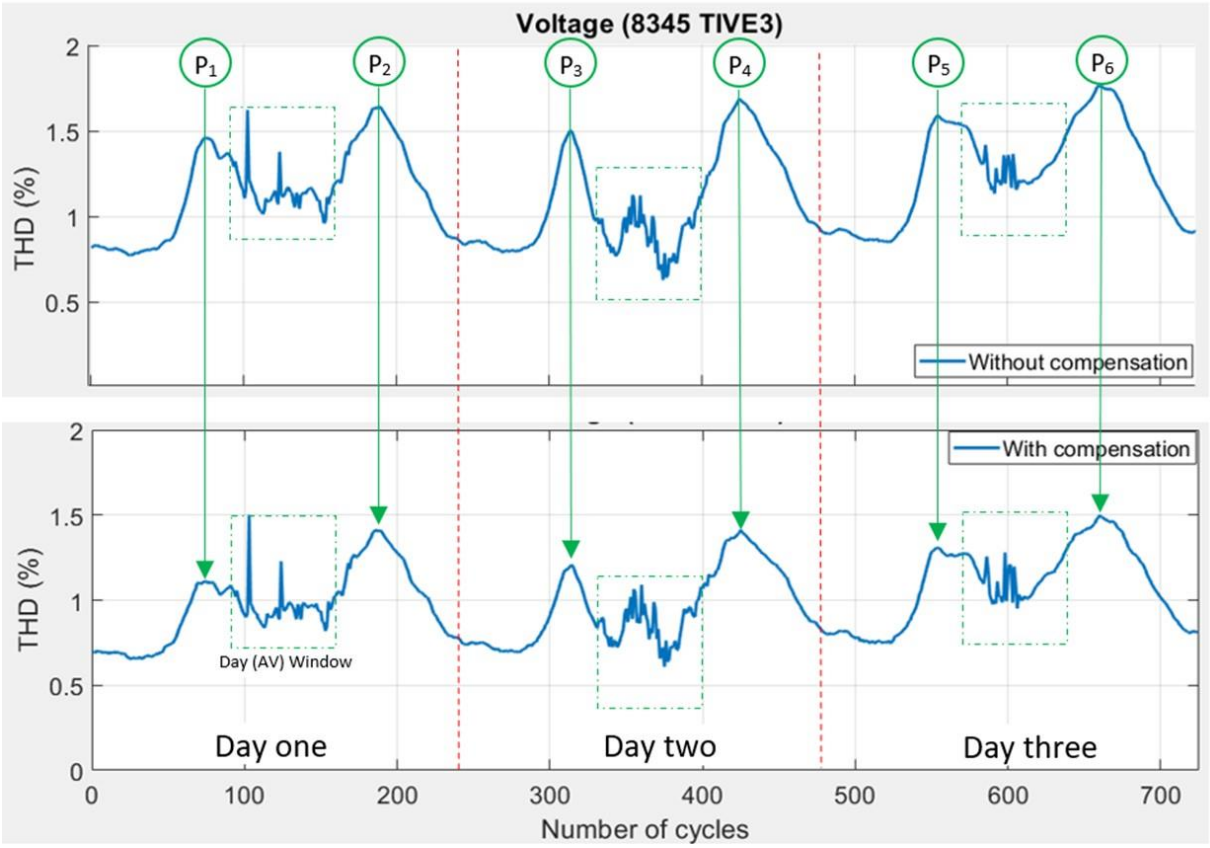


*Figure 29 Voltage THD calculation at TIVE3 over three-day period with and without compensation*

*Table 11 TIVE3 voltage THD calculation comparison*

| Data points | without comp. | With comp. | Voltage THD reduction (%) |
|---|---|---|---|
| P1 ( X73) | 1.457 | 1.119 | 33.8 |
| P2 (X186) | 1.637 | 1.417 | 22 |
| P3 (X314) | 1.498 | 1.208 | 29 |
| P4 (X424) | 1.688 | 1.413 | 27.5 |
| P5 (X555) | 1.59 | 1.314 | 27.6 |
| P6 (X660) | 1.764 | 1.496 | 26.8 |
| | | | |
| Day one (Av) 9am-4pm | 1.2432 | 1.0026 | 24.06 |
| Day two (Av) 9am-4pm | 0.9131 | 0.8464 | 6.67 |
| Day three (Av) 9am-4pm | 1.3439 | 1.1403 | 20.36 |
| Total Three Days average | 1.1594 | 1.0003 | 15.91 |

## 3.4.4. Transformer Losses

The primary effect of introducing AF operation on the transformer operation is a possible increase in copper losses. The losses are proportional to the square of the rms current at fundamental frequency as well as at harmonic frequencies. In this case the copper losses can be estimated using:

$$P_{Cu} = I_1^2 R_1 + I_5^2 R_5 + I_7^2 R_7 + I_{11}^2 R_{11} + I_{13}^2 R_{13}$$

where the respective frequency dependent resistance values are calculated based on international best practice described in [6].

Figure 30 introduces the calculation of copper losses with and without compensation for the fundamental current, for harmonic currents and as total losses. It is if importance to note that transformer losses increase with the extra duty of compensation active (compare bottom two charts). However, under the majority of operating circumstances, the losses are lower than the full fundamental rated load losses of the transformer (around 5 kW). It is possible to observe short periods where losses exceed the rated level by up to 15% and this is thought to be acceptable as it is unlikely to drive temperature increase resulting in hotspots that would accelerate insulation ageing. This aspect is further investigated during WP3 eventually resulting in the introduction of an additional limiter in the controller such that transformer losses never exceed rated losses.

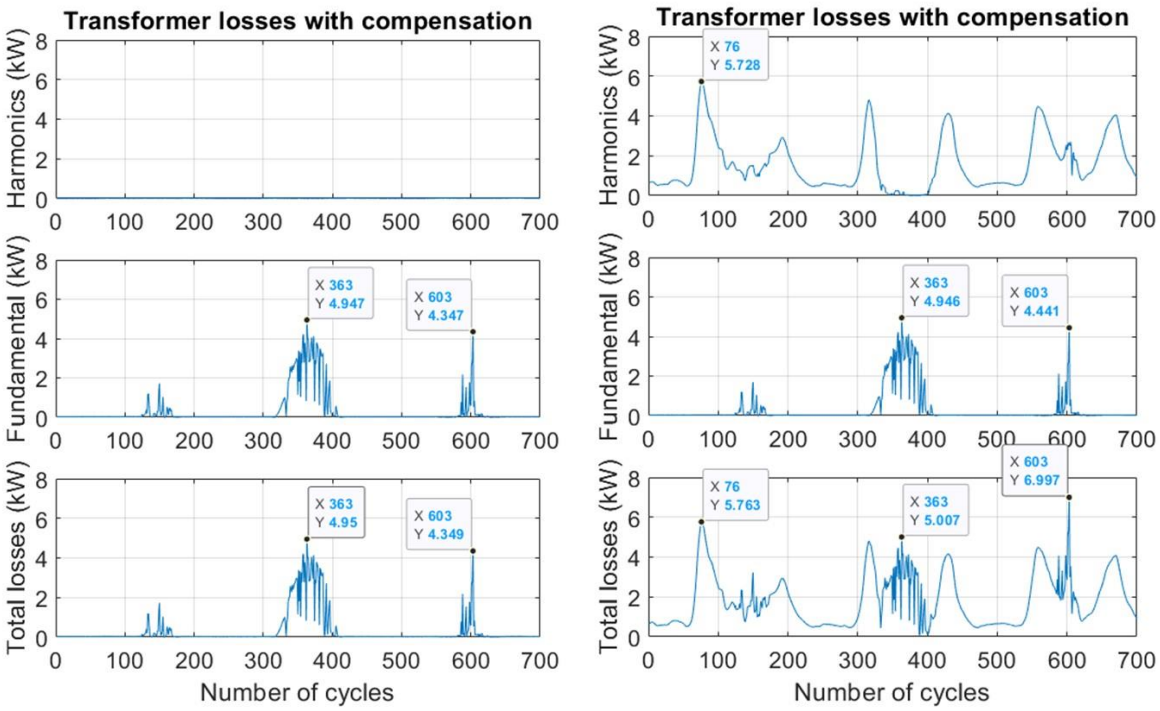


*Figure 30 Transformer loss calculation with and without compensation*

## 3.5. Lessons Learned in WP2

Challenges that shaped WP2 were mainly encountered during the design stage of the control algorithm. Most of the issues faced were part of the detailed design process, analytical difficulties and as such extremely difficult to anticipate from the onset. Hence, they were dealt with as and when they were encountered. The following list provides some of the key issues encountered and the solutions implemented in order to overcome the issue.

- Oscillations in harmonic reference signal: this was observed during extraction of harmonic content and was identified to be due to the low pass filter which then was replaced with a better performing notch filter.
- Overcompensation under high irradiance: high compensation currents were detected which was identified as a result of high gain coefficient being used. This was overcome by introducing

an automatic gain based on a look-up table to use high gain only at times of low irradiance, i.e. more capacity.

- Poor compensation at higher harmonic order: it was observed that the 11$^{th}$ and 13$^{th}$ harmonic compensation was less effective than 5$^{th}$ and 7$^{th}$ due to using the same gain values. This was resolved by setting separate gain values for group of harmonics thus providing even further versatility on the controller.
- PI controller not effective in harmonic generation: use of the PI controller in generating compensating harmonics was seen to be poor as the PI is more appropriate for the fundamental frequency. This was resolved by replacing the PI controller with a number of PR controller (one for each harmonic group).
- No compensation under unbalanced conditions: initial design attempts showed lack of compensation under unbalanced conditions. Additional filtering was added to cater for unbalanced situations (this was only done for the 5$^{th}$ harmonic positive sequence).
- Burst of harmonic injections: this was noticed to be coming out of the inverter due to sudden changes in the gain value to keep up with the level of change due to irradiance. To resolve this, the irradiance profile was modified using a rate limiter and a hold to ensure that gain is held for 10 minutes.

## 3.6. WP2 Concluding Remarks

The primary objective of WP2 was to develop a control algorithm for one of the PV inverters such that it can provide AF duty in addition to the main task of active power generation.

An algorithm has been developed to compensate the feeder current taking into account all the specified requirements. The algorithm includes an automatic gain functionality where the harmonic gain changes according to the control parameters (for example capacity to compensate).

Initial functional test proved the correct operation of the algorithm in terms of compensation it provided under specified harmonic distortions.

Further operational tests aiming to demonstrate the functionality and performance of the algorithm has taken place. In these tests it was possible to demonstrate that the control algorithm is successful in reducing the level of harmonic distortion under varying levels of active power generations and with changing system harmonic levels. Whilst the algorithm is performing AF operation it was also demonstrated that the operation is not causing any adverse issues with the network or other plant items (for example losses on inverter transformer is within levels of rated losses).

A key observation was that the algorithm was more effective in mitigating harmonic distortion under low-irradiance conditions. This was expected as the controllers give priority to fundamental active power generation. With sufficiently low irradiance levels, the controller (based on single inverter) will mitigate up to 8.7 A of harmonic current to virtually zero. In terms of voltage THD, a key performance indicator, it was observed that reduction of up to 34% is possible.

Overall, it was concluded that the developed algorithm is robust and effective enough to be applied to multiple inverters in order to have a coordinated compensation strategy on network harmonic distortion.

# 4. Work Package 3

WP3 is aimed to build on the control algorithm developed in WP2 by employing the same control in multiple inverters. Location of the inverter and the measurement points ($P_1$ to $P_7$ and L) used for feedback purposes are shown in Figure 31. The figure also shows location of scenarios (S1-S8) used for robustness checks later in section 4.2.1. Two different approaches were taken in employing all the inverters:

- Inverters operating independently
- Inverters operating in coordination

In the first case, each inverter unit is controlled as an independent AF without any coordination or communication between the inverters.

In the second approach, a coordinated control between the inverters is employed in order to optimise compensation based on the source of harmonic currents and on the power generated by each power PV inverter.

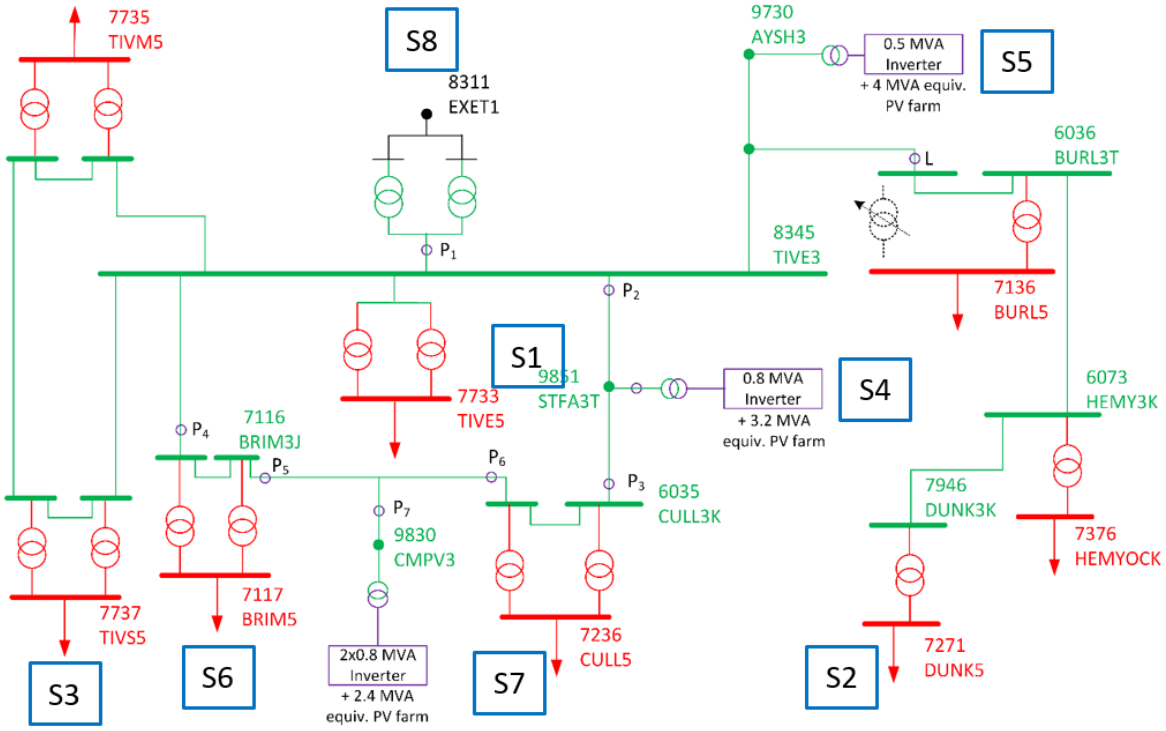


*Figure 31 Inverter, feedback measurement points and operational scenario locations*

Furthermore, based on the outcome and observations during the tests, further improvements were applied to the control algorithm.

## 4.1. Independent Inverter Operation

For independent operation each inverter operated on its own without any further information being fed.

**Ayshford PV farm** has a single inverter (0.5 MVA inverter and an additional 4 MVA equivalent PV farm) and this was already utilised for the development of the control algorithm as explained in WP2. As the harmonic flow is unidirectional from the 11 kV loads at BURL5 to the upstream system, the algorithm development was rather simplified and the best feedback point for harmonic reference currents were

on the radial network load current (point L in Figure 31). The deployment of the AF algorithm at Ayshford PV farm was the subject of WP2 and it has been documented in the WP2 report extensively.

**Cullompton PV farm** has two inverters (0.8 MVA each and an additional 2.4 MVA PV farm) and the choice of the point for current measurement was the first priority as it is not as simple as the case in Ayshford. Various points in the network, $P_1$, $P_2$, $P_3$, $P_5$, and $P_6$ in Figure 31 were tested for the most appropriate location by evaluating the level of compensation achieved in various scenarios. It was found that $P_1$, was the optimum point.

Tests were conducted to check that the control algorithm will run for the first inverter and upon the success of it, the control algorithm was deployed to the second inverter also with similar stability checks indicating good operation.

**Stoneshill PV farm** has a single inverter (0.8 MVA with an additional 3.2 MVA PV farm) and a similar approach to Cullompton PV farm was followed. Best feedback point found to be $P_1$.

A complete simulation was carried out over the three-day period with each inverter providing an independent compensation under the following conditions:

- The feedback load current measurements points are chosen as $P_1$ for Stoneshill and Cullompton inverters, and L for Ayshford inverter.
- All loads and harmonics ($5^{th}$, $7^{th}$, $11^{th}$, and $13^{th}$) are included.
- Background distortion from upstream 132k V network is included.
- Inverter irradiance and load variations are modelled according to the measured data.
- Automatic gain applied to all inverters.

The performance of this operation is checked via the voltage THD at TIVE3 BSP and the whole trend is depicted in Figure 32 where compensated level shows substantial reduction. Analysis of the shown spot and average (applying to between 9am to 4pm) checks are included in Table 12. As seen in the table, operation of all four inverters bring a major reduction compared for example with the operation of a single inverter at Ayshford when it was tested under the conditions in WP2. Details of the WP2 results are included here for comparative purposes.

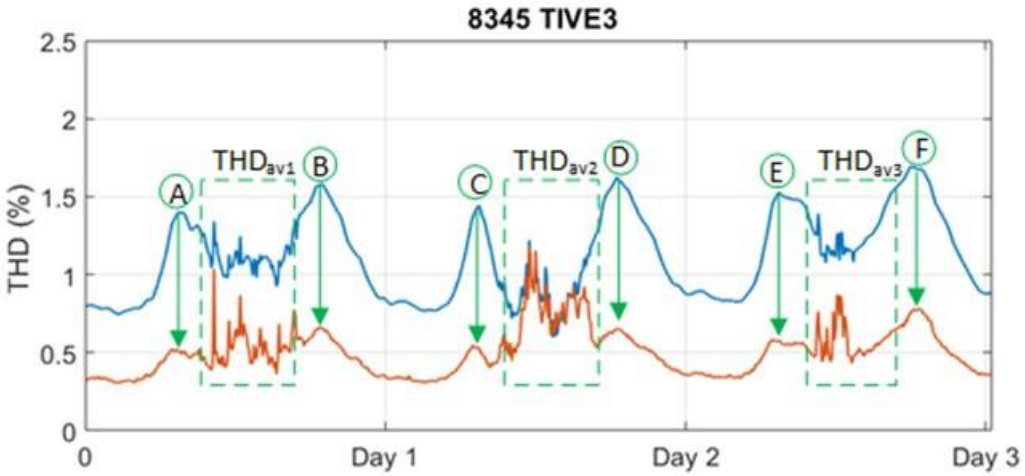


*Figure 32 Voltage THD at TIVE3 with (orange) and without (blue) AF compensation with uncoordinated inverters*

*Table 12 Voltage THD analysis comparison for uncoordinated inverter operation*

| THD voltage profile point | THD no compensation | THD independent compensation | Reduction (%) | Reduction (%) against WP2 results |
|---|---|---|---|---|
| A | 1.45 | 0.51 | 64.8 | 22.9 |
| B | 1.64 | 0.65 | 60.3 | 13.4 |
| C | 1.50 | 0.54 | 64.0 | 19.4 |
| D | 1.69 | 0.66 | 60.9 | 16.3 |
| E | 1.59 | 0.58 | 63.5 | 17.4 |
| F | 1.76 | 0.77 | 56.2 | 15.2 |
| $THD_{av1}$ | 1.24 | 0.56 | 54.8 | 19.4 |
| $THD_{av2}$ | 0.91 | 0.79 | 13.1 | 7.3 |
| $THD_{av3}$ | 1.34 | 0.80 | 40.2 | 15.1 |

**Lack of Correlation between current and voltage THD**

Peculiarities were observed during the analysis of the simulation results. When harmonic compensation was implemented, at some busbars, there was an increase of current distortion, while at the same time there was a reduction of voltage THD as can be seen in Figure 33. In the figure, compensation is activated at 4am and as expected at location $P_1$ (see Figure 31 for locations) voltage THD decreases with a decreasing current THD. However, the behaviour at location $P_5$, is the opposite: the voltage THD decreases while the current THD increases.

This behaviour was pinned down to the PR controllers within the control algorithm where the open-loop frequency response of the inverter indicates very high admittance at the tuned harmonics ($5^{th}$, $7^{th}$, $11^{th}$, and $13^{th}$). The implication of this is that a reduction of the system impedance takes place when the inverter is connected to the system and the AF algorithm is activated. The effect can be seen in Figure 34 with a drop in impedance at the frequencies of interest. Frequency scans run at other locations indicates that the impact of the PR controller decreases with the increase of electrical distance from the inverter, thus matching the behaviour observed during the tests.

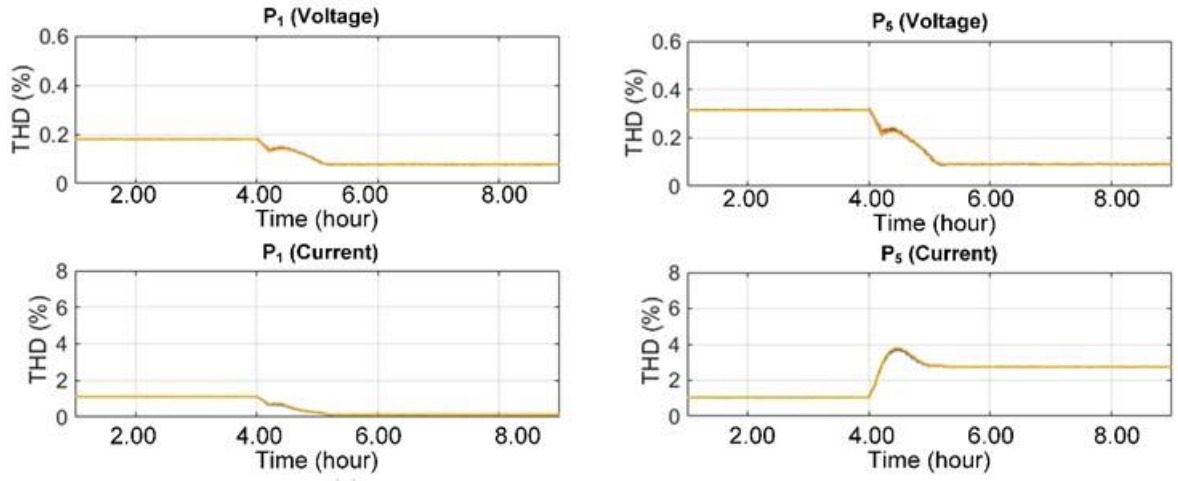


*Figure 33 Voltage and current THD at two points on the Tiverton network*

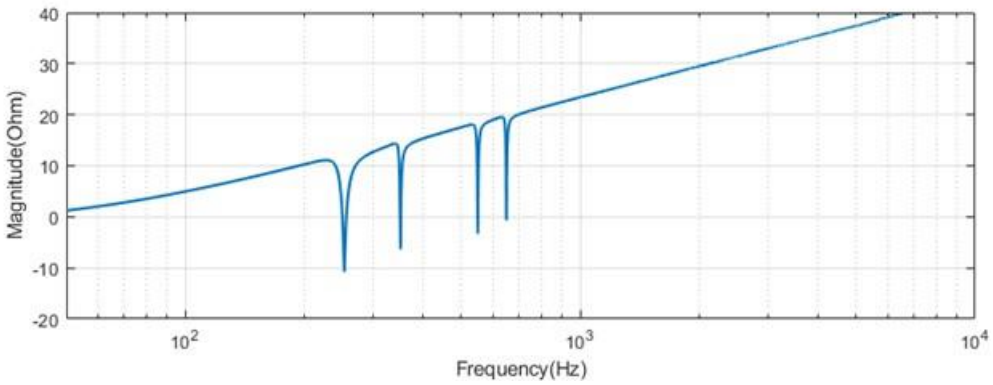


*Figure 34 System impedance seen from Cullompton with AF in operation*

## 4.2. Coordinated Inverter Operation

To determine the best coordinated approach, various current measurements at different point were tested as input current into the inverters AF controller as given in Table 13. Actual points are shown in Figure 31.

*Table 13 Load current feedback point options (see Figure 31 for point locations)*

| | Current measurement point | | |
|---|---|---|---|
| | Cullompton | Stoneshill | Ayshford |
| Case 0 | $P_1$ | $P_1$ | L |
| Case 1 | $P_1$ | $P_1$ | $P_1$ |
| Case 2 | $P_1$ | $P_2$ | L |

During the investigation, it was observed that Ayshford takes an increased harmonic compensation duty when $P_1$ is used as measurement feedback point. At this point all harmonic load current within TIVE3 network are included and not just the radial load harmonic current when point L was used. A similar behaviour was observed for Stoneshill when comparing $P_1$ against $P_2$ (Case 0 and Case 1 against Case2). This is turn helps Cullompton to have a reduced duty when Ayshford and Stoneshill use $P_1$ as the measurement point. Inverter currents for all three inverters under all three cases are shown in Figure 35.

Comparison of the voltage THD at TIVE3 for the three cases is shown in Figure 36 and it is clear that the Case 1 provides the best overall mitigation which corresponds to the common current feedback point of $P_1$.

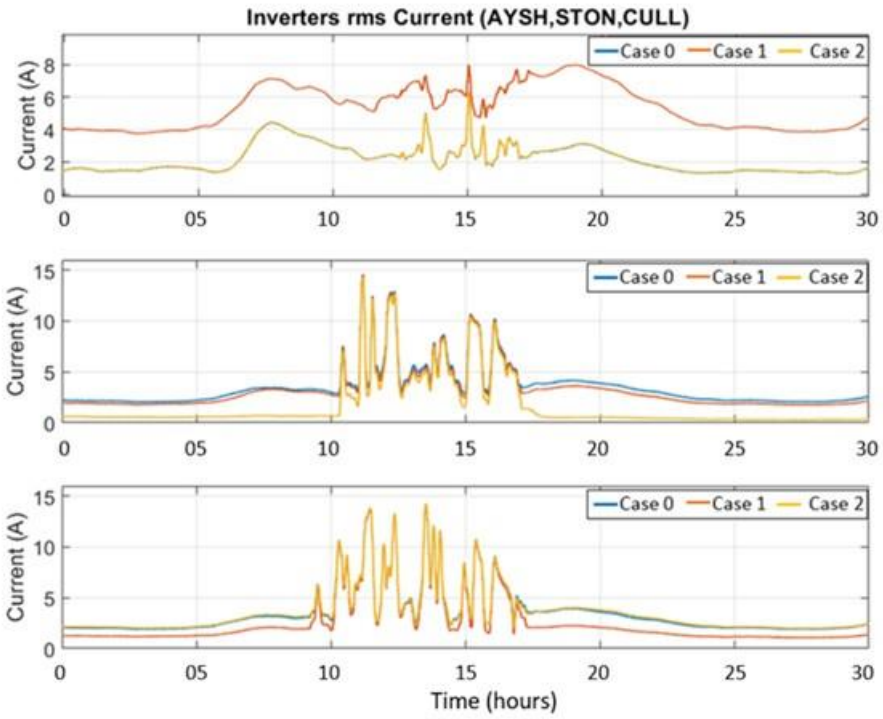


*Figure 35 Ayshford, Stoneshill and Cullompton inverter currents for the cases listed in Table 13*

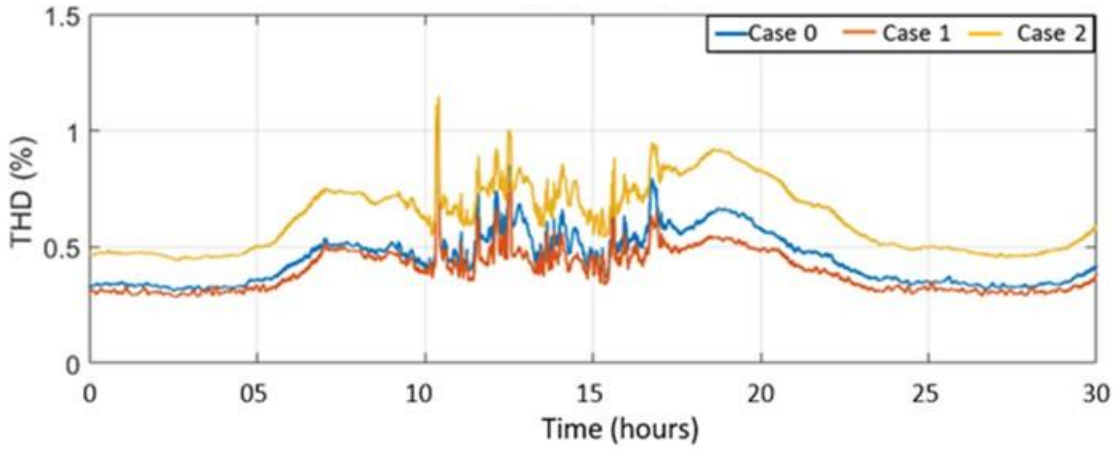


*Figure 36 Voltage THD at TIVE3 with different load point measurement coordination*

## 4.2.1. Robustness tests on control location.

Few validity tests were carried out to check the robustness of the overall control scheme under the following operational scenarios (shown in Figure 31):

S1. Disabling harmonic injection at TIVE5.
S2. Doubling harmonic injection at DUNK5.
S3. Modifying the phase shift of harmonic injection at TIVS5.
S4. Disabling compensation from Stoneshill inverter.
S5. Setting Ayshford inverter fundamental current to zero.
S6. Disconnecting BRIM5 load and harmonic injection.
S7. Switching off the second inverter at Cullompton.
S8. Doubling the upstream voltage distortion.

The tests were performed in the same simulation run (total of 55 hours) by applying each scenario under different time periods. Inverter currents and the voltage THD at TIVE3 were monitored. The latter is shown in Figure 37 and the results are all in line with the expectations. For example, reduced compensation is expected during S4 and S7 as one inverter is out of action.

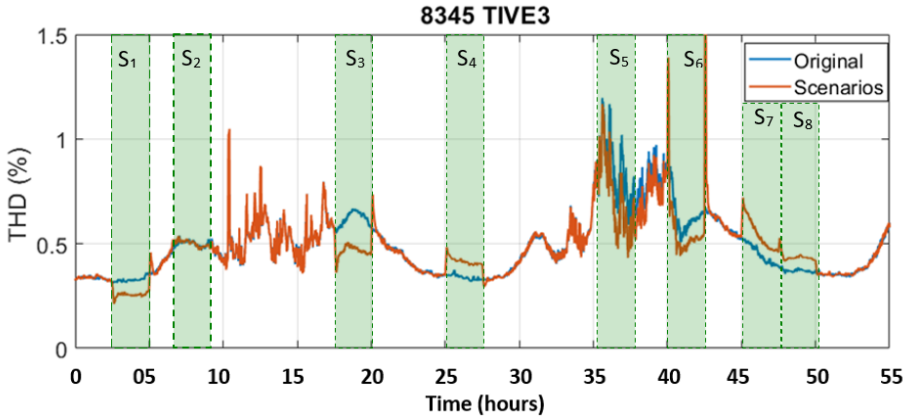


*Figure 37 Voltage THD at TIVE3 under robustness scenario testing*

## 4.2.2. Robustness tests under network contingency.

Some further test under contingency conditions were carried out, where the loop including Cullompton PV farm and Stoneshill PV farm was open at different points:

- $P_2$ open between 6.00 and 10.00,
- $P_3$ open between 12.00 s and 16.00,
- $P_4$ open between 18.00 and 22.00.

Voltage THD results at TIVE3 indicated that during the first contingency (open circuit at P2) the THD increases. This increase was identified to be due to an amplification at 15$^{th}$ harmonic current when system measured voltage is used in the controller without any filtering. A Low Pass Filter (LPF) to the input voltage resolved this resonance condition. Overall, the contingencies have not resulted in any unstable operation of the controller since the LPF was introduced.

## 4.2.3. Comparison with and without compensation, and co-ordinated compensation.

At the final stage, a comparative analysis covering all three days of the simulation was carried out using P1 as the coordinated feedback point. Results are shown in Figure 38 and include the results of the independent operation also.

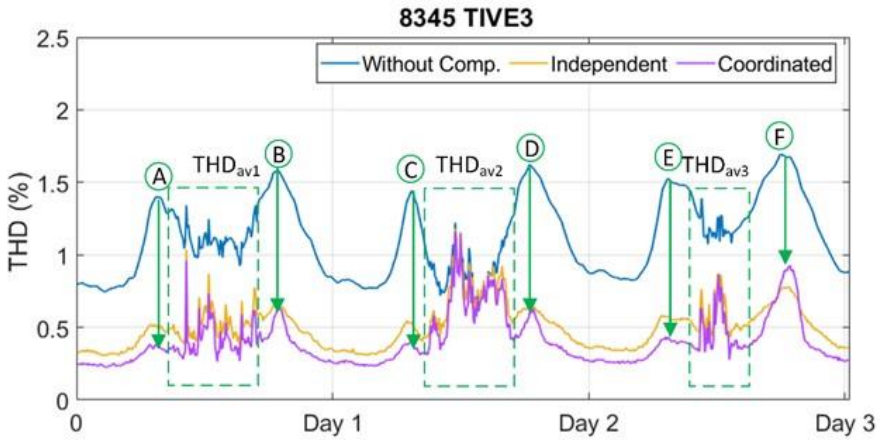


*Figure 38 Voltage THD at TIVE3 with and without AF compensation with coordinated inverters*

Analysis of the shown spot and average (applying to between 9am to 4pm) checks are included in Table 14. As seen in the table, operation of all four inverters using a coordinated approach bring further reduction of voltage THD compared to uncompensated but more importantly also to uncoordinated case.

*Table 14 Voltage THD analysis comparison for coordinated inverter operation*

| THD voltage profile point | THD no compensation | THD coordinated compensation | Reduction (%) | Reduction against independent compensation (%)) |
|---|---|---|---|---|
| A | 1.45 | 0.45 | 69.0 | 64.8 |
| B | 1.64 | 0.62 | 62.1 | 60.3 |
| C | 1.50 | 0.38 | 74.6 | 64.0 |
| D | 1.69 | 0.62 | 63.3 | 60.9 |
| E | 1.59 | 0.42 | 73.6 | 63.5 |
| F | 1.76 | 0.91 | 48.4 | 56.2 |
| $THD_{av1}$ | 1.24 | 0.49 | 60.6 | 54.8 |
| $THD_{av2}$ | 0.91 | 0.72 | 21.1 | 13.1 |
| $THD_{av3}$ | 1.34 | 0.76 | 43.3 | 40.2 |

## 4.3. Refinement of the Control Algorithm

As a result of the tests applied above, further refinements were applied to the control algorithm, with the effect of improving its performance. The core of the algorithm is the same as developed in WP2, with the following elements added:

- A low-pass filter to remove high-frequency components from the voltage signal measured on the power grid.
- A transformer losses coefficient ($k_t$) that curtails the harmonic currents to ensure that the transformer losses are kept equal to or below the rated value.

### 4.3.1. LPF Implementation

The initial control algorithm did not include any filtering of the input voltage, and therefore any distortion created could amplify and feed into the controller creating additional amplified distortion. This was observed for the 15$^{th}$ harmonic under some contingencies and to eliminate the condition, an LPF was added.

The LPF in effect eliminates any distortions on the measured voltage signal above the cut-off frequency (1 kHz), and this in turn stops the inverters in producing any excess harmonics due to internal control loops and switching processes. The MATLAB/Simulink implementation is shown in Figure 39.

### 4.3.2. Transformer Loss Coefficient Implementation

During AF operation there is a possibility of the step-up transformer connected to the inverter exceeding the rated values of losses. Losses in this context refer to copper losses that are due to the fundamental and harmonic currents. To overcome this possibility, a harmonic current limiter was introduced to the control algorithm based on the following principle

$$I_1^2 R_1 + I_5^2 R_5 + I_7^2 R_7 + I_{11}^2 R_{11} + I_{13}^2 R_{13} \leq I_{1,rated}^2 R_1$$

where, $I_1$, $I_5, I_7, I_{11}$, and $I_{13}$ represent the fundamental and 5th, 7th, 11th and 13th rms current, respectively; $R_1$, $R_5, R_7, R_{11}$, and $R_{13}$ are the frequency dependent resistances of the transformer. Following few mathematical manipulations, the expression can be rewritten as a coefficient in the *dq* reference frame as follows:

$$k_t = \sqrt{\frac{1 - i_d^2}{(i_{d4}^2 + i_{q4}^2)\, r_5 + (i_{d6}^2 + i_{q6}^2)\, r_7 + (i_{d12}^2 + i_{q12}^2)\, r_{13}}}$$

This coefficient was then used as a multiplier to adjust the level of injected harmonics. Various checks and tests were run to establish a range for $k_t$ such that the losses are kept within the rated value.

Transformer losses were calculated for all three inverter locations and established that the loss coefficient is works by keeping the overall losses within the rated values Calculation for the Ayshford inverter is shown in Figure 40 as an example where the rated losses are indicated with the horizontal red line.

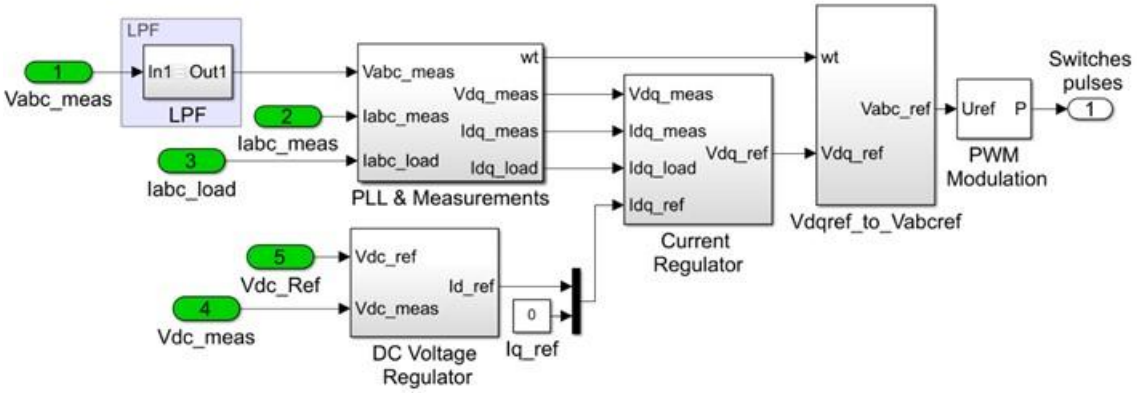


*Figure 39 Revised key components of the AF control algorithm*

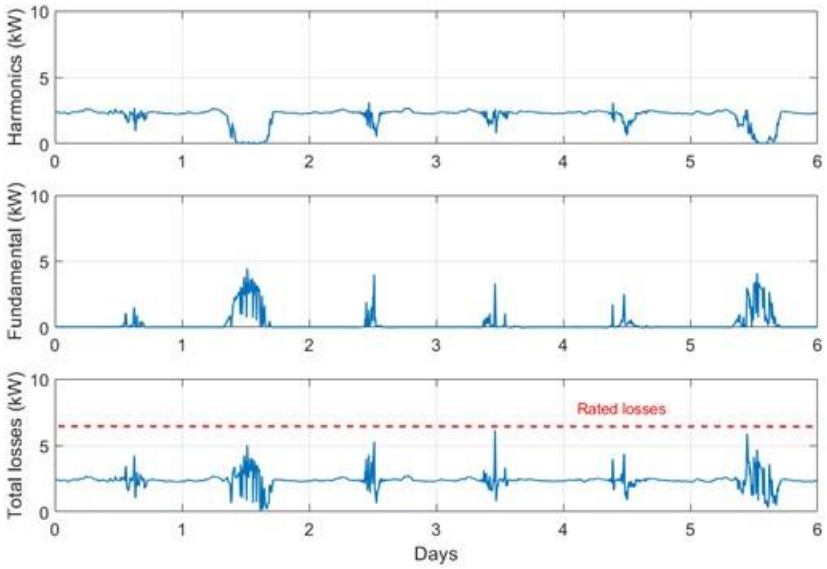


*Figure 40 Ayshford inverter transformer losses*

## 4.3.3. Updated Control Algorithm

The implementation of these two additions is shown as highlights in the overall control structure presented in Figure 41.

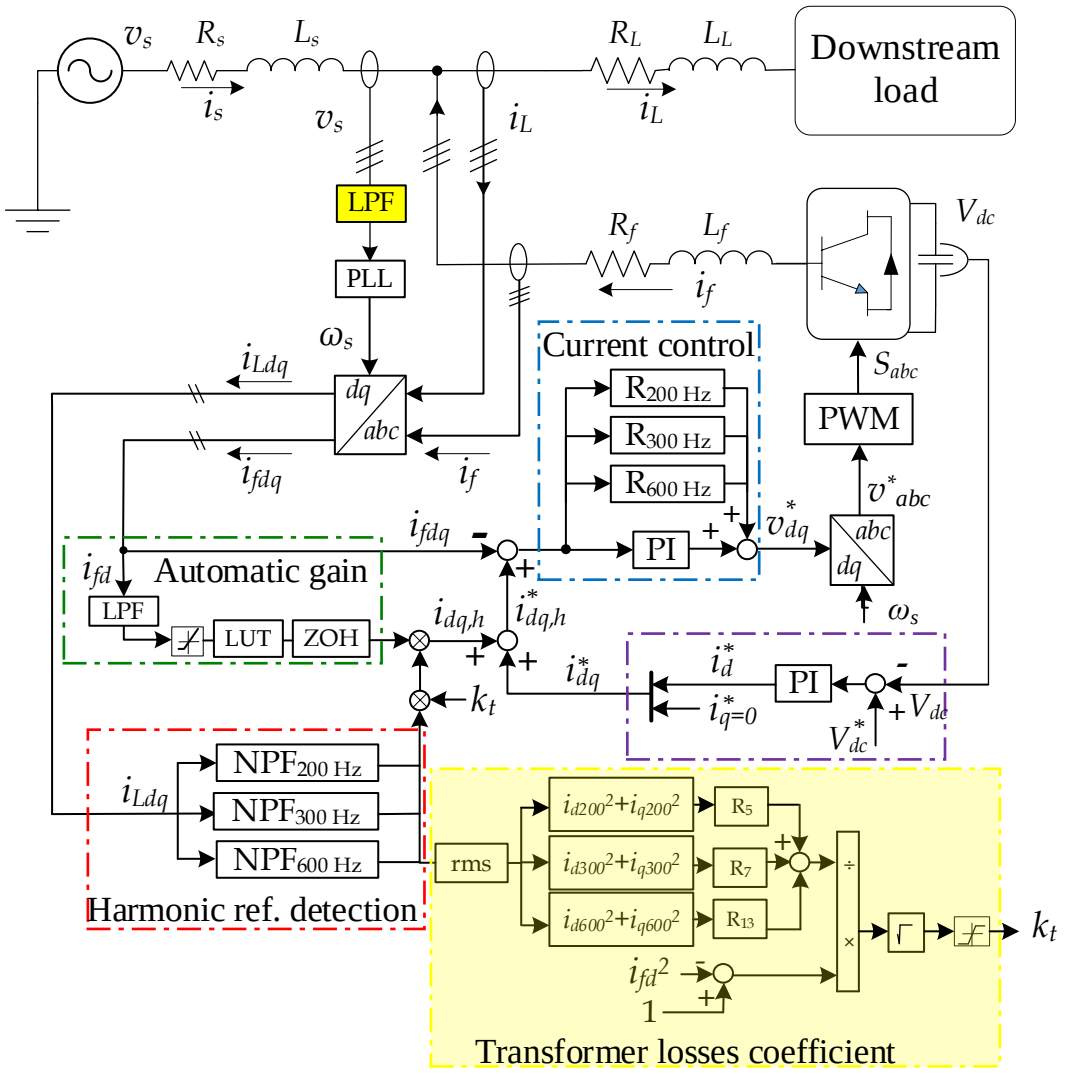


*Figure 41 Updated control algorithm schematic*

## 4.3.4. Combined Algorithm Performance

With the updated control algorithm, the studies performed earlier over three days were repeated and the voltage THD at TIVE3 was analysed to check control algorithm performance with the results as shown in Figure 42 (indicated as "With $k_t$ threshold = 0.3") and with further analyses presented in Table 15 against the previous results. One immediate observation was that during the day the peak reduction is less with the coordinated and inclusive of $k_t$ coefficient in relation to just coordinated compensation. At night-time, the THD values with the latest version of the algorithm ($k_t$ lower threshold equal to 0.3) were slightly lower.

The results shown indicate that coordinated operation leads to the best compensation in terms of reduction of THD peaks and THD average value during the day. However, this approach does not introduce any protection on the possibility of exceeding losses with the inverter transformers.

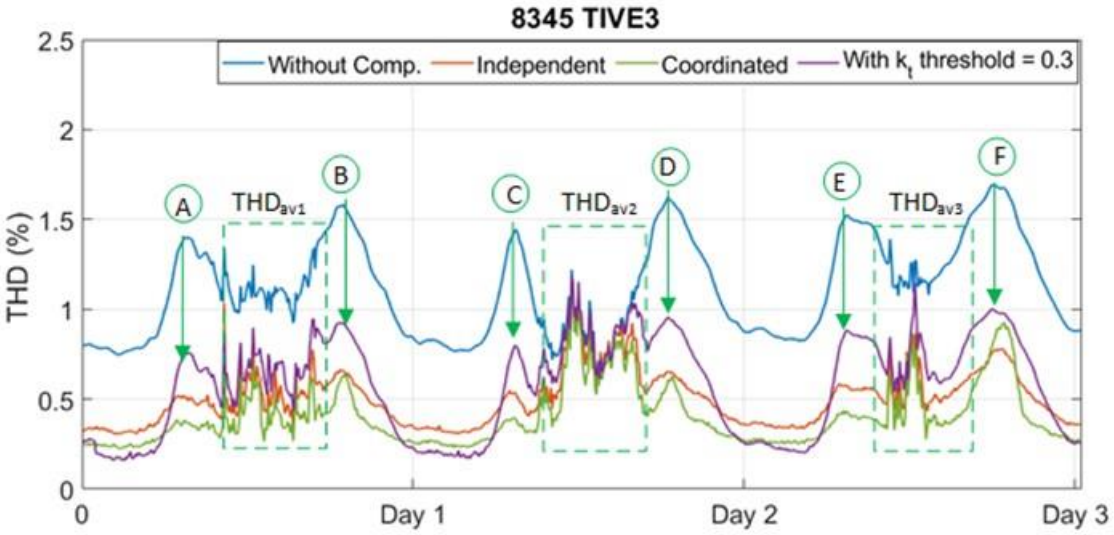


*Figure 42 Voltage THD at TIVE3 comparing updated control algorithm with previous strategies*

*Table 15 Voltage THD analysis comparison with updated control algorithm*

| THD voltage profile point | Voltage THD reduction (%) | | |
|---|---|---|---|
| | Independent compensation | Coordinated compensation | Coordinated With $k_t$ = 0.3 |
| A | 64.8 | 69.0 | 47.5 |
| B | 60.3 | 62.1 | 43.9 |
| C | 64.0 | 74.6 | 47.3 |
| D | 60.9 | 63.3 | 44.9 |
| E | 63.5 | 73.6 | 45.2 |
| F | 56.2 | 48.4 | 43.7 |
| $THD_{av1}$ | 54.8 | 60.6 | 37.0 |
| $THD_{av2}$ | 13.1 | 21.1 | 7.7 |
| $THD_{av3}$ | 40.2 | 43.3 | 40.0 |

## 4.4. Lessons Learned in WP3

The critical take away lessons in WP3 relate to the point of feedback measurement and the impact of inverter impedance on equivalent network impedance:

- While the best current measurement point for the normal operation of the network under study is identified as a single point, it is possible to have multiple measurement points with the possibility to modify them, depending on system operating conditions or other events (for example, faults on a feeder). This could be done automatically as part of wider control strategy such as communication between different controllers and/or other network control/automation parameters. Using a different current measurement point will change the duty on each inverter (both increase and decrease is possible).
- The inverters have an impact on the equivalent network impedance, in particular at the frequencies of current injection, due to a combination of inverter output filter and control loops. The inverter equivalent impedance changes when AF operation is activated, due to the

introduction of additional control loops, compared to normal operation. This could result in a misleading observation between voltage and current harmonics at different locations on the network. The impact decreases with increased electrical distance in the point of interest (i.e. where equivalent network impedance is calculated).

## 4.5. WP3 Concluding Remarks

The primary objective of WP3 was to extend the control algorithm built and tested in WP2 to multiple inverters on a distribution network to perform harmonic mitigation in a coordinated and optimised way.

The control algorithm developed in WP2 was implemented at other locations within the given network. The operation of the inverters as AF was optimised such that the most effective and coordinated mitigation is employed. This involved checking multiple feedback points to test the optimum operation.

Further control functionalities were introduced in the form of a low pass filter and a limiter. The former resolves any internal harmonic amplification while the latter allows the overall transformer losses not to exceed rated values, thus introducing protection against overheating. This protection was achieved by a coefficient with threshold limits multiplied with harmonic reference currents. However, introducing this loss coefficient results in loss of some AF compensation capacity.

While implementing the control algorithm over multiple inverters, the robustness and the stability of the algorithm was tested under various scenarios. Results indicated possible issues with excitation of a resonance by small inverter harmonic current which was resolved with the introduction of a low pass filter.

# 5. Work Package 4

WP4 involves experimental validation of the developed control algorithm by means of testing it in a laboratory environment using real time digital simulations technique. A key component if this was to compare the results with those obtained in WP2. To achieve this objective, the following stages were taken forward:

- Preparation of the model and the control algorithm for the HIL testing
- Validation of the algorithm using HIL testing

The following sections describe the two stages taken forward in the execution of this WP.

## 5.1. Laboratory Equipment and Model Preparation

### 5.1.1. Laboratory Setup

For the HIL tests, the experimental test bench shown in Figure 43 has been set up at a laboratory environment. The two main components are an OPAL-RT emulator (OP5600) and a Taraz Technologies three-phase inverter (PELab). The OPAL-RT emulator is used to run the network model and the PELab hosts and runs the control algorithm developed for this project for one of the inverters. The two units are connected such that it is possible to transfer the analogue signals from the OP5600 to the PELab, and the digital signals from the PELab to the OP5600. The approach therefore is suitable for a 'hardware in the loop' analysis, the hardware being the inverter.

A laptop is interfaced to both OP5600 and PELab allowing the execution of simulation and saving the variables of interest. Two oscilloscopes are also connected, one to each of OP5600 and PELab providing immediate visualisation of selected waveforms.

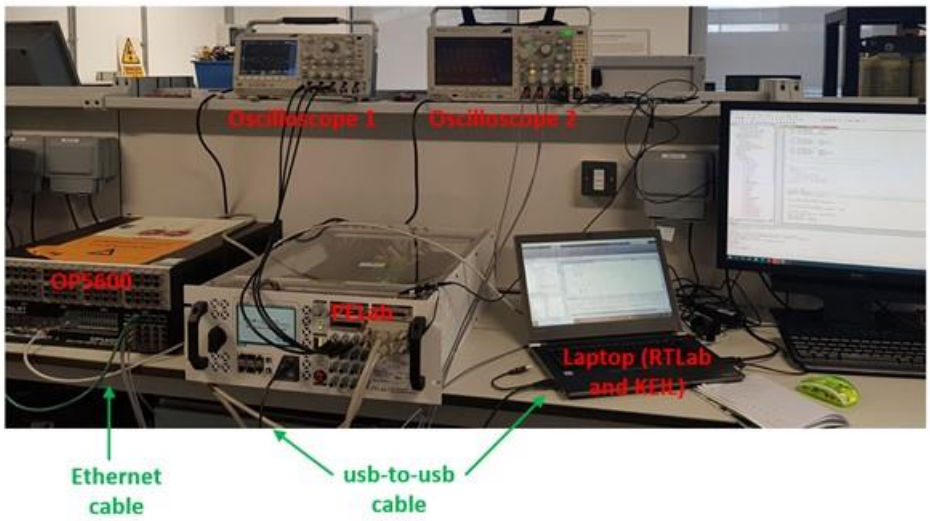


*Figure 43 Experimental test bench*

RT-LAB, used to manage the main simulation model loaded on the OP5600 is fully integrated with MATLAB/Simulink and allows Simulink models to be imported and edited in RT-LAB. Following manipulations required by the OP5600 environment, the model developed in the previous work packages were loaded into OP5600. Some further simplification required for processing and adjustment on sampling time have also been introduced such that no overruns are observed.

PELab was also programmed with the developed control algorithm using the applicable software coding (KEIL software and C-code). Some adjustments to the analogue input signals due to scaling

between PELab and OP5600 were introduced. Similarly, the digital output of the PELab were processed in an intermediate step in order to provide switching signals to OP5600.

With all the adjustments and fine tunings, the laboratory setup was checked whether it would be possible to see a current being injected by the inverter. Figure 44 shows Ayshford inverter current while injecting all four harmonic currents of interest indicating correct operation of the setup.


*Figure 44 Ayshford invert current while generating all harmonics of interest*

## 5.1.2. Network Model Setup

The network model was integrated into the experimental analysis by importing it into RT-LAB. The network model initially was set up as a static model where loads use fixed values. However, in order to replicate results of WP2 where the entire three-week period was simulated, the model had to be made suitable to import the measurement datasets into the network and use as a dynamic model.

Two separate import blocks had to be used for the measurements as the two sets (SCADA and PQ data) use different resolution (half hourly versus 10 second). Three different adjustments were made to the model setting in order to run the dynamic model in real time using the measured data.

**Time step of the simulation had to be increased** from the relatively small value of 8 µs in Simulink to 100 µs to accommodate the large network and large data set due to the speed limitation introduced by OP5600.

**Interpolation was introduced into the SCAD dataset** as the 30-minute resolution corresponding to 0.1 s in simulation time results in a step change of demand which in turn provides significantly different results from WP2 simulations results. Interpolation resulted in gradual change ad in return a behaviour similar to WP2 and WP3 results.

**Duplication of PQ data points was introduced** to eliminate a shift in the result introduced by data mismatch to real time simulation time step. PQ data has a resolution of 10 s corresponding to 0.556 ms in simulation which cannot be used by RT-LAB as it is not an integer multiple of the simulation time step (100 µs). An acceptable resolution of 0.5 ms is introduced but this leads to a shift in the results that was resolved by duplicating one point at every ten points of the PQ data. This duplication does not introduce any deviation from realistic operating points but allows a much more meaningful comparison of the results with previous work package results. A schematic relating to the mapping of SCADA and PQ data is shown in Figure 45 where the magenta colour identifies the duplicated point. Figure 46 shows comparison over a single day and for the entire period the time covered by the

Simulink simulations (indicated as simulation), OPAL-RT simulations without adjustment (shown as RT) and the OPAL-RT simulations with adjustments (shown as modified RT).

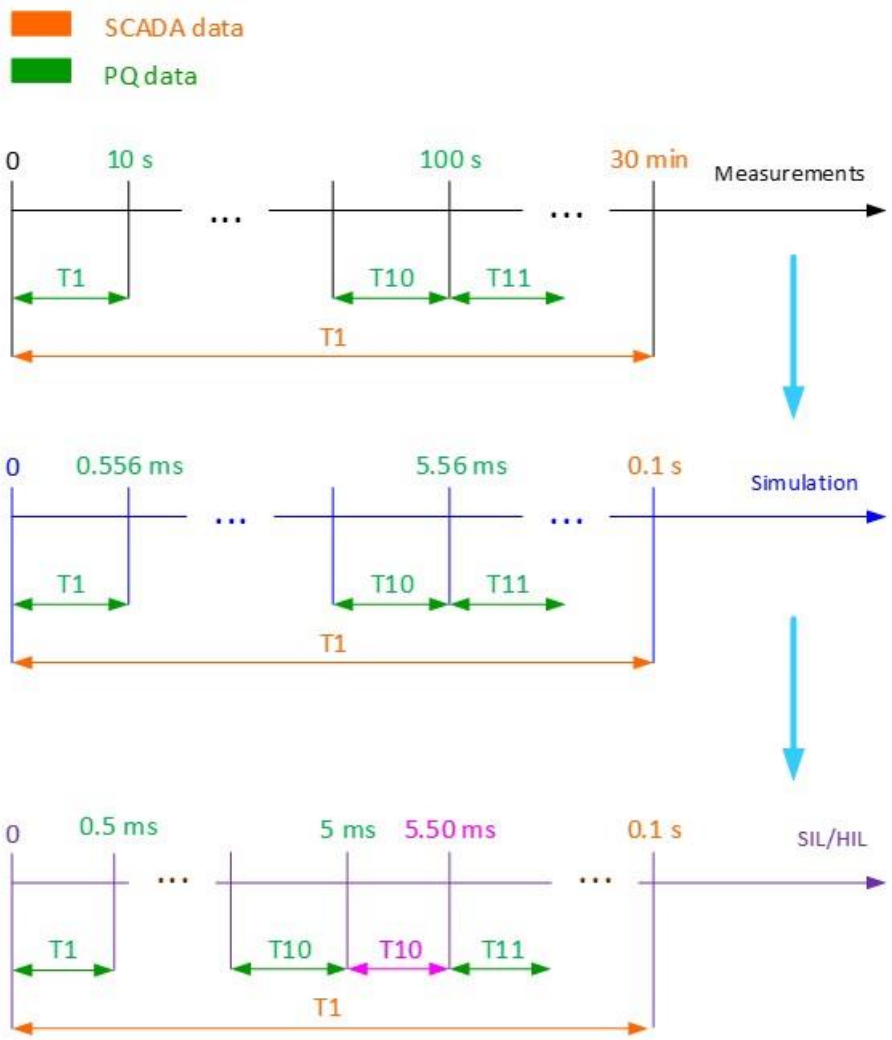


*Figure 45 Mapping of SCADA data and PQ data in different domains*

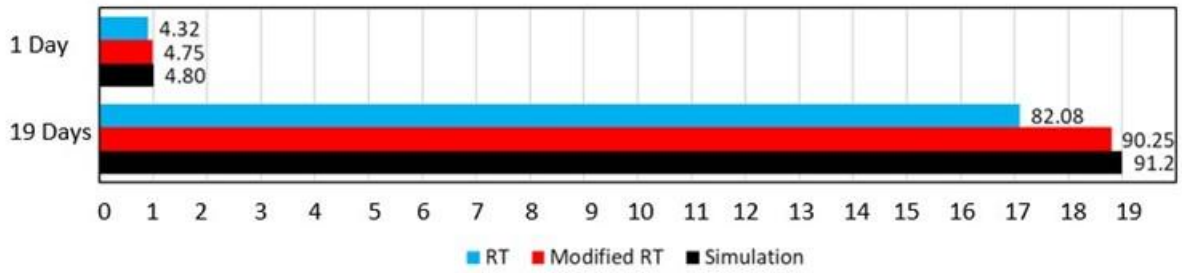


*Figure 46 Comparison of total simulation times*

It is worth noting the importance of these adjustments with reference to simulated variables to understand the effect on the results. As it can be seen in Figure 47, significant error is introduced due to the time shift between the two sets of results, whereas in Figure 48 this time shift is eliminated, and the two sets of results are significantly more aligned.

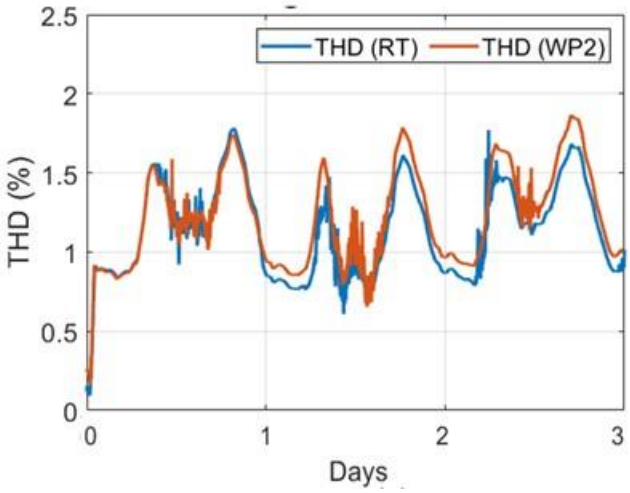


*Figure 47 Voltage THD at TIVE3 comparison of OPAL-RT results without model adjustment with WP2*

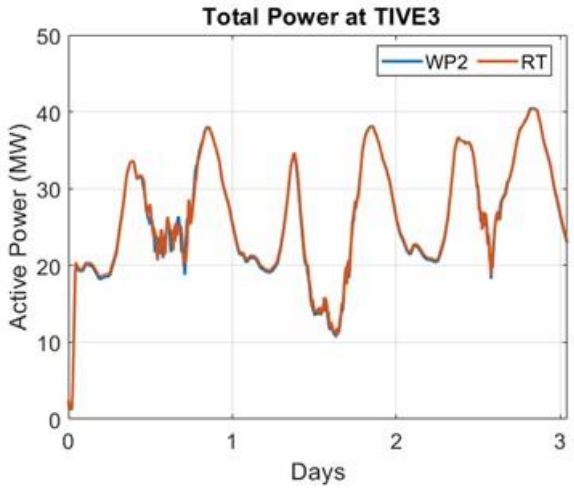


*Figure 48 Total power TIVE3 comparison of OPAL-RT results without model adjustment with WP2*

The introduction of dynamic modelling into real time digital simulation led to inverter instability and eventually tripping of the inverter. Some of the issues identified related to the inverter code and these were rectified by improving the generation of switching pulses. Although this improved the overall runtime of the simulation, it didn't eliminate the issue of premature simulation termination altogether. It was observed that the issue was mainly due to the computational effort required to run the network in real time, and accumulation of delays in the transmission of analogue and digital signals between OP5600 and PELab This then led to further modifications in the network model that was achieved by compacting the model to create a simplified representation.

The most important point on the simplified representation was that it should allow to test the prosed functionality as was developed. The simplified model was obtained by combining all SCADA data into an equivalent load at TIVE5 as seen in Figure 49 with an increased transformer rating. The PV farms at Cullompton and Stoneshill were also represented by means of equivalent models. This simplification of the network model however required verification to check whether the results of the previous work packages could still be matched.

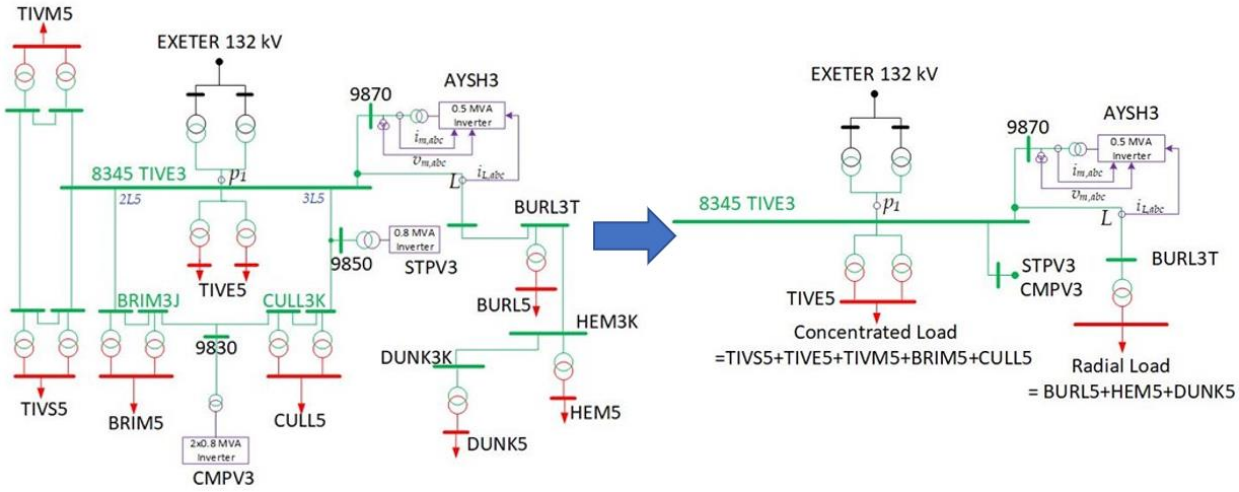


*Figure 49 Reducing the size of network model for HIL analysis*

Following initial checks, it was found that using the simplified model resulted in a higher active power measurement at TIVE3. This was to be expected as losses associated with lines and transformers were no longer in the model. To cater for this the overall power was reduced by 8% to match with the results of WP2 at TIVE3 (the level may sound higher than usual, but the overall simplification includes five load locations being brought under one while trying to replicate SCADA readings). Further verification was conducted comparing voltage THD at TIVE3 as presented in Figure 50. Some discrepancies are present, particularly towards the end of the observation period due to the mismatch between the WP2 results that replicate PQ data resolution and the adjusted RT-Lab simulations. To improve this, "zero" values were added to the PQ data at the end of day 5, day 10 and day 15, all corresponding to night-time period where there is no PV generation. This does not result in any introduction of error but improves the match significantly as presented in Figure 51. Further detailed comparison is provided in Table 16 and based on these results it was concluded that the simplified network model provides a reliable representation of the network model to perform HIL simulation and subsequently compare them with the results of WP2.

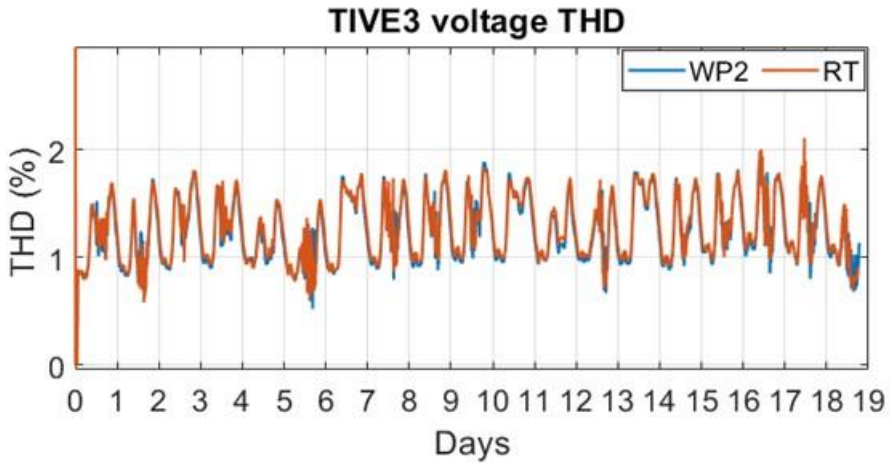


*Figure 50 Voltage THD comparison between WP2 results and simplified real-time model (no compensation)*

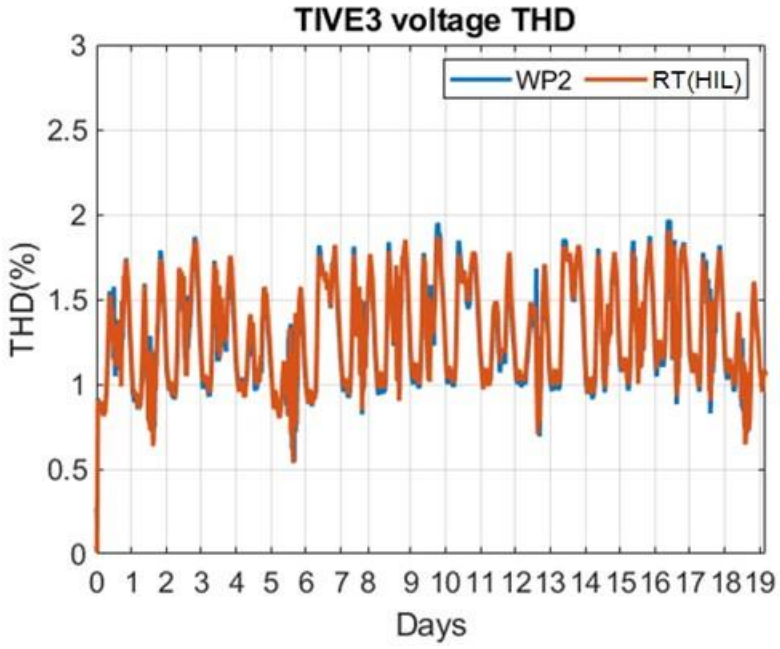


*Figure 51 Voltage THD comparison between WP2 results and simplified real-time model (no compensation) following further adjustments*

*Table 16 Detailed comparison of voltage THD at TIVE3 between WP2 and simplified RT (without compensation).*

| | WP2 (THD) for entire period (%) | RT (THD) for entire period (%) |
|---|---|---|
| Mean | 1.24 | 1.25 |
| Max | 1.93 @ t= 78.9s (16 d, 9:30 h) | 1.99 @ t= 78.9s (16 d, 9:30 h) |
| Min | 0.57 @ t= 26.90s (5 d, 14:40 h) | 0.60 @ t= 26.90s (5 d, 14:40 h) |

## 5.2. HIL Testing

With all the checks on the models complete the experimental setup was utilised to perform the HIL testing. The initial approach was to test the whole setup under static test conditions where the network model for the Tiverton network is static providing a stable and controlled environment to check the functioning of the algorithm. The algorithm was verified for normal operation, i.e., generation of active power where it is effectively providing a sinusoidal current output. This was followed by switching the compensation in where the inverter is providing harmonic current output in addition to the fundamental. Figure 52 shows a screen capture from the oscilloscope covering both modes of operation for the inverter under test.

With the confidence that the algorithm is functioning properly under static model conditions, the model was replaced with the simplified dynamic model for the final part of HIL testing.

Initial attempts indicated oscillatory response in THD suggesting that the voltage waveform may be the origin of the issue. This observation was similar to what was experienced in WP1 where the issue was resolved with the introduction of a shunt resistance in parallel with dynamic load. A similar solution was introduced here, making sure that the final value of the resistor (10 kΩ in this case) has no effect on study result. The introduction of the shunt resistor provided significant improvement in

getting close match between the results of WP2 and that of HIL. However, discrepancies were still observable as shown in Figure 53.


*Figure 52 Inverter current showing switching instance into compensation mode.*

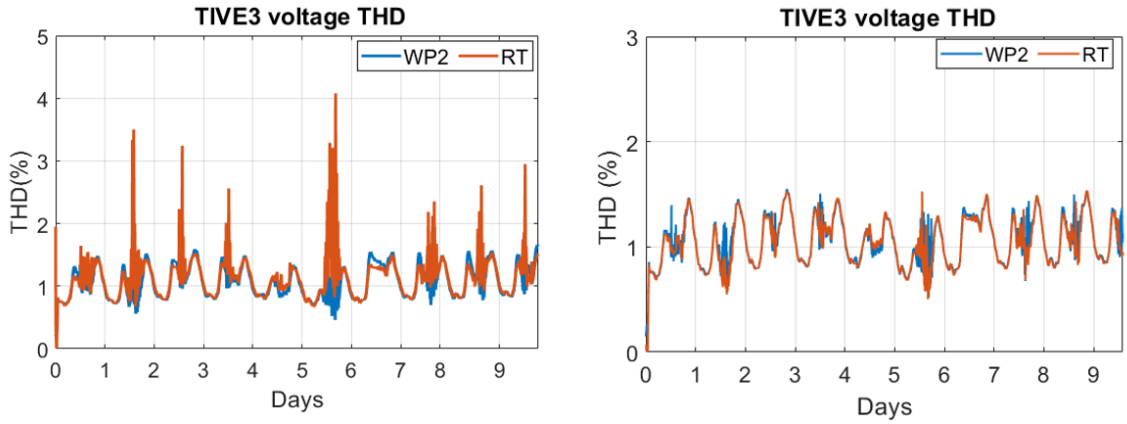


*Figure 53 Voltage THD comparison before (left) and after (right) the addition of the shunt resistor.*

Further improvements were made via revisions on the automatic gain functionality. It should be recalled that an automatic gain function was introduced in WP2 that regulates the fundamental current flow in the inverter and to avoid rapid changes in harmonic injection the value of the gain was updated every 10 minutes. This time period corresponds to 33.33 ms in the model environment (0.1 s simulation time is equivalent to 30 min real time) which is not an integer multiple of the HIL simulation time step (100 µs). The automatic gain update was increased from 10 min to 15 min corresponding to 50 ms and making it an integer multiple of the HIL simulation time step. In addition, the input current signal to the automatic gain is filtered so that only the fundamental is passed.

With all the improvements introduced, HIL results are compared to WP2 results as shown in Figure 54, Figure 55 and Figure 56.

The variation of the inverter current in Figure 54 is caused by a combination of varying irradiance and varying harmonic injection and overall, there is a very close correlation between the two plots.

Figure 55 shows the comparison for one of the phase currents under two conditions, a daytime operation when there is slightly more deviation between the two plot and a night-time operation when

there is much more agreement. The deviation during the daytime operation is primarily due to the automatic gain response (the difference of 10 min versus 15 min update) when the level of irradiation changes and the gain has to adjust on a continuous basis. During the night-time there is no active power generation, and the inverter is continuously on harmonic compensation duty with automatic gain hardly changing.

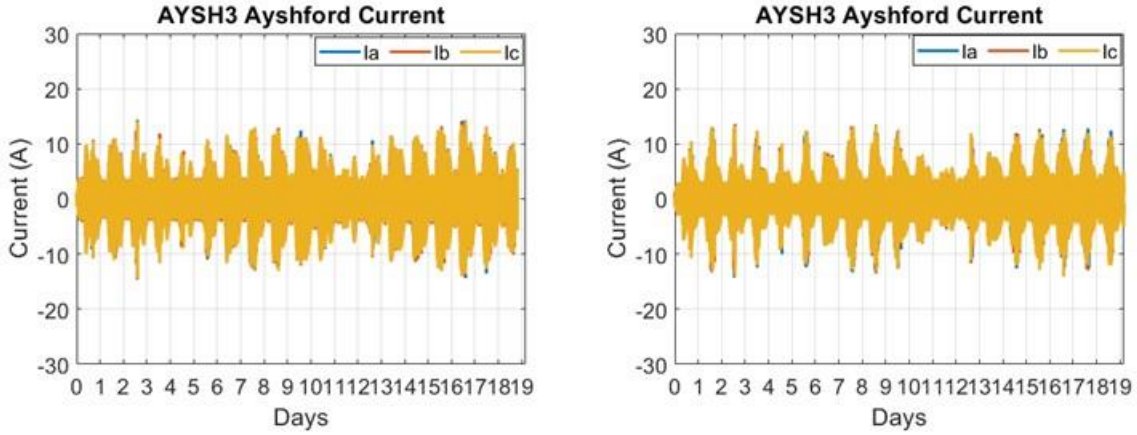


*Figure 54 Inverter current with AF operation WP2 results (left) vs HIL (right)*

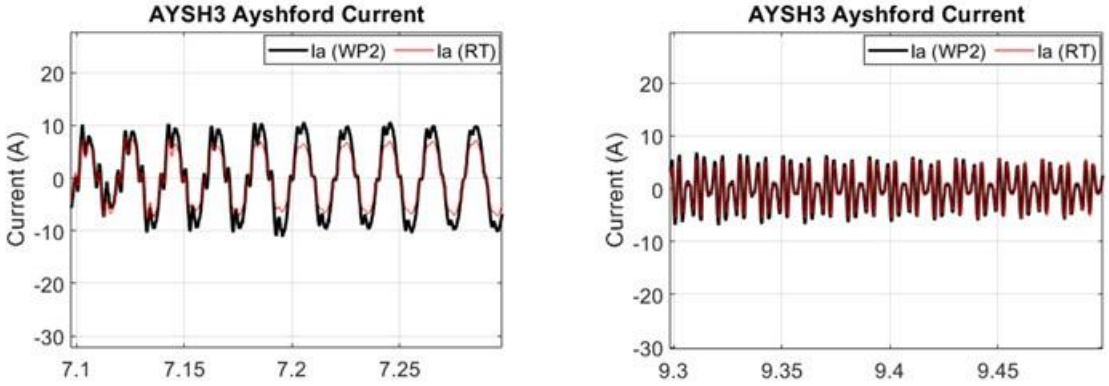


*Figure 55 Comparison of inverter current with compensation during daytime (left) and night-time (right) operation*

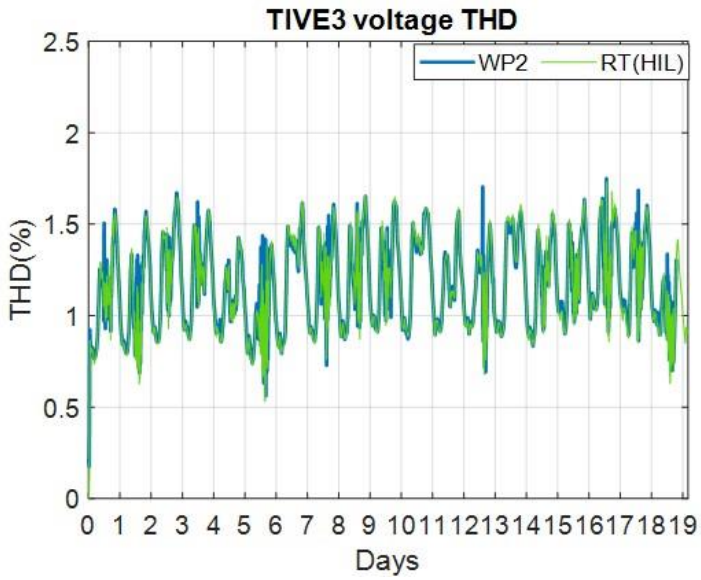


*Figure 56 Voltage THD at TIVE3 comparison between WP2 and HIL*

Finally, in Figure 56, voltage THD at TIVE3, the key performance indicator is compared with an extremely good match. It is almost impossible to have an exact match here due to differences in sampling time, modifications introduced in the PQ data and network reduction. It is possible to see that WP2 results show spikes around midday for day 1 and between day 12 and day 13, that are not present in HIL. These differences are due to the different tuning of the automatic gain, and increased sampling time in the HIL tests. HIL results for example do not show rapid variations due to the increase sampling time compared with WP2. A more quantitative analysis and comparison is provided in Table 17 showing average, minimum and maximum values for the THD with a very close match between simulations from WP2 and HIL tests.

One further HIL test relating to transformer losses was checked and results were compared with those from WP2. Figure 57 shows the comparison of transformer losses between the HIL results and the WP2 simulation results. In general, the results are well aligned and where differences are present those are mainly due to the underlying reasons given for previous comparisons, i.e., the sampling time, refitting of the PQ data and modification in the automatic gain tuning. It should be noted that the rated transformer losses are 5.7 kW and it can be clearly observed that this level in exceeded a few times in both analysis (WP2 and HIL) due to the lack of transformer loss coefficient in the control algorithm (implemented later in WP3).

*Table 17 Detailed THD analysis comparison between WP2 and HIL*

| | WP2 (THD) for 19 days (%) | HIL (THD) for 19 days (%) |
|---|---|---|
| Mean | 1.05 | 1.05 |
| Max | 1.68 @ t=79.3 s (16 d, 13:30 h) | 1.67 @ t=79.3 s (16 d, 13:30 h) |
| Min | 0.53 @ t=27.2 s (5 d, 14:00 h) | 0.54 @ t=27.2 s (5 d, 14:00 h) |

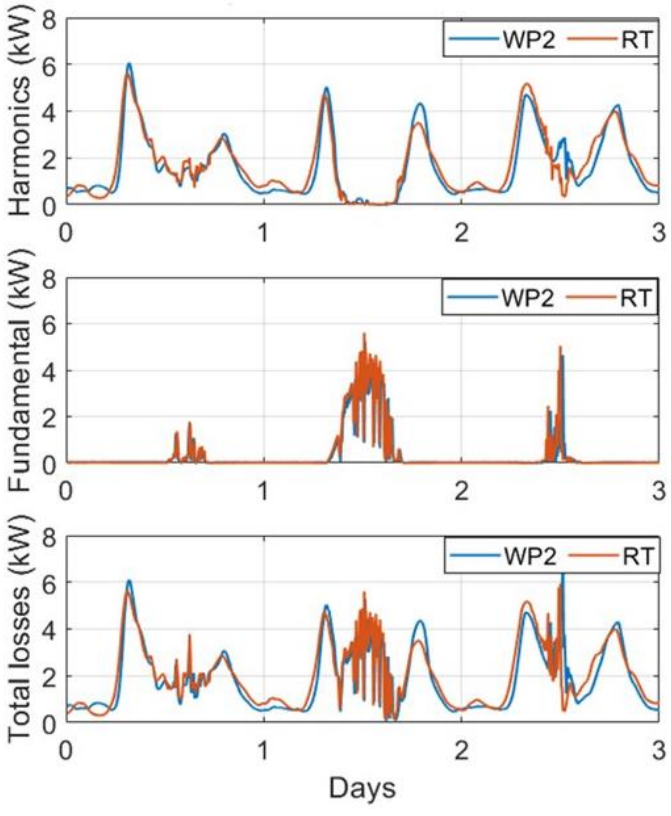


*Figure 57 Comparison of transformer losses between WP1 and HIL tests*

## 5.3. Lessons Learned in WP4

Key learning point in WP4 relate to the capability of the equipment used for real time digital simulations.

1- A small time-step of 8µs were used initially in MATLAB/Simulink simulations due to the presence of short lines. The lowest time-step the emulator OPAL-RT 6500 could only accommodate was established to be 20 us. However even with this lowest time-step overruns (effectively a mismatch between simulator operations/calculations and the real time) were observed during the real-time simulations. Real-time simulations are considered erroneous in the presence of overruns. Hence, the time-step of the digital simulator had to be increased to 100 µs to overcome the issue associated with overruns.

2- Real-time simulation uses discrete time-steps where at each time step the simulator reads input and produces output by solving the model equations and then waits for the start of the next step. This suggests that any external connection is sampled once at the beginning of each simulation step and hence external data (such as PQ and SCADA) had to be an integer multiple of the digital simulator time-step.

3- The size of the Tiverton network proved to be large for the digital simulator. This was unexpected considering that larger network models are solved on such platforms routinely. Abrupt simulation stops were observed and eventually when the model was heavily simplified, it was possible to run complete simulations.

## 5.4. WP4 Concluding Remarks

The main objective of WP4 was to test the developed control algorithm in a laboratory environment using real-time digital simulation approach.

Difficulties were encountered during the process of real-time simulator setup that included overruns, mismatch of external data sampling, mismatch of control algorithm time critical items (such as updating of the automatic gain functionality). These differences resulted in output parameters (such as the THD) to be observed in an oscillatory or time shifted fashion. Corrective attempts were introduced such that the overall results are affected only at minimum level.

Inclusion of corrective modification resulted in very close agreement between the output of WP2 simulations and the HIL test output proving that the algorithm developed is effective in reducing the harmonic distortion present in the network of study.

# 6. Learnings, Conclusions and Recommendations

This section provides a high-level summary of the main learning and conclusions points from all the work packages along with recommendations for further work.

## 6.1. Key Learnings

During the execution of the project several difficulties were encountered, and these were resolved using best engineering approach.

The key elements were all listed in the work packages, but it is of importance to draw attention to key takeaways that could have been anticipated at earlier stages:

- It would be advantageous to know and understand the limitations of the analysis platform at the onset of the project. Suitability of PSCAD, RSCAD and RTDS either stand alone or in combination with OPAL-RT 6500 and/or MATLAB/Simulink could have been examined to find the best alternative.
  - Lack of tap changer in transformer models in MATLAB/Simulink
  - Lack of frequency dependency modelling for most of the power network elements in MATLAB/Simulink.
  - Inadequacy of the emulator OPAL-RT 6500 in accommodating small integration time-steps.
  - Capability of the emulator OPAL-RT 6500 to accommodate only a very small network model.
  - Observation of numerical stability issues with the time domain solvers in both MATLAB/Simulink and OPAL-RT 6500.
  - The need to introduce a magic resistor to the model both in MATLAB/Simulink and HIL simulations (however it should be noted that the effect of this is negligible on study results and is a common approach employed in numerical integration studies).
- Knowledge of time samplings on measured data needs to be known or planned in advance of starting the project execution.
  - Input data utilised for models based on SCADA and temporary PQ monitors were observed to be in significantly different time resolution.
  - Time resolution of measured data was not suitable for the discrete time-steps in the real-time simulator.
  - Observation of the overall simulation being computationally intensive. This type of difficulty would be seen in other electromagnetic transient analysis environments also with the main driver being the time step and the overall duration of the simulation time. The largest time step that can be used is dictated by the model characteristics and not much can be done about it. The duration of the simulation is split into multiple parts so that simulation time is shortened, and the data generated can be handled easily.

There were other important key learning points that were overcome during the execution of the project in effect resulting in a more optimised control algorithm design. These can be listed as:

- Introduction of design modifications within the control algorithm for continuous improvements.
  - Replacement of the low pass filter with a better performing notch filter to avoid oscillations in harmonic reference signal.
  - Introduction of an automatic gain such that the inverter is not overloaded under high irradiance conditions.
  - Separation of gain from applying to a single harmonic to a grouping of harmonics thus providing balanced compensation between harmonic orders.

- Introduction of a PR controller instead of a PI controller while generating harmonics for injection.
- Introduction of additional filtering to cater for unbalanced conditions in the harmonics.

A final point to make regarding learnings relate to observations during the execution of the project.

- Whilst an optimum location of feedback measurement was established for normal operation, it is possible to have multiple measurement points with the possibility to modify them, depending on system operating conditions or other events (for example, faults on a feeder).
- The inverters have an impact on the equivalent network impedance, in particular at the frequencies of current injection, due to a combination of inverter output filter and control loops.

## 6.2. Project Conclusions

The main objective of the project was to develop an algorithm that can improve the network's harmonic levels by controlling existing distributed generation inverters. An extended objective was to apply this to multiple inverters as well as testing the performance of the algorithm in a laboratory environment.

Following a comprehensive literature review, a project model was established and validated in MATLAB/Simulink environment during WP1. This environment provided a realistic representation of the actual network for the purpose of developing and testing harmonic mitigation algorithms to be overlaid on already included PV inverter models.

In WP2 a control algorithm was developed to compensate harmonics measured on a feeder considering all the specified requirements. The algorithm includes an adaptive compensation via an automatic gain functionality. The developed algorithm proved to be successful in reducing the level of harmonic distortion under varying levels of active power generations and with changing system harmonic levels. An important aspect shown was the lack of any adverse effect from the controller whilst performing AF functionality. A key observation was that the algorithm was more effective in mitigating harmonic distortion under low-irradiance conditions. This was in line with the expectations as the controllers give priority to fundamental active power generation during high irradiance conditions. During simulations, it was observed that reduction of up to 34% in voltage THD was possible leading to the conclusion that the developed algorithm is robust and effective enough to be applied to multiple inverters to have a coordinated compensation strategy on network harmonic distortion.

The control algorithm developed in WP2 was then implemented at multiple inverters within the network under study in WP3. Optimisation on the operation of the inverters as AF was carried out by testing multiple feedback points such that the most effective and coordinated mitigation is employed. This results in further improvement on the voltage THD. Additional control functionalities were introduced in WP3 in the form of a low pass filter and a limiter. During the tests to check the robustness and the stability of the algorithm, excitation of a resonance by small inverter harmonic current was observed and was resolved with the introduction of a low pass filter. A limiter was introduced that allows the overall transformer losses not to exceed rated values, thus introducing protection against overheating. Introducing this loss coefficient functionality however resulted in reduction of AF compensation capacity. However, a reduction of up to 47% in voltage THD was still possible.

Real-time digital simulation tests under laboratory conditions took place in WP4. During the setup of the whole process, difficulties were encountered that included overruns, mismatch of external data sampling, mismatch of control algorithm time critical items (such as updating of the automatic gain functionality). These differences inhibited like for like comparison of the output parameters (such as the THD) as oscillatory or time shifted waveforms were observed. Corrective attempts were introduced

such that the overall results are affected only at minimum level. The overall simulations then indicated a very close agreement between the output of WP2 simulations and the HIL test output.

The overall conclusion following the successful results of WP4 is that the control algorithm developed is effective in reducing the harmonic distortion present in distribution networks.

## 6.3. Recommendations for Future Work

Overall, the project should be classified a success story as all objectives have been fulfilled. However, based on the learning points and the observation during the execution of the project, it was possible to identify future work items that will bring more engineering and scientific knowledge to the existing level of understanding. Various opportunities for further work can be listed as:

- Introduce communication functionality between inverters. Although the current project found an optimum working pattern, each inverter can be controlled in automatically coordinated fashion such that the level of gain in each is adjusted considering not just its own capacity but also of the other inverters. This could be further enhanced by adjusting gain on harmonic group basis in both directions in multiple inverters, i.e., different inverters providing their compensation capacity for different group of harmonics.
- Introduce adaptability to change feedback points as required. This could be done automatically as part of wider control strategy such as communication between different controllers and/or other network control/automation parameters. Using a different current measurement point will change the duty on each inverter (both increase and decrease is possible).
- Extend HIL testing to include multiple inverters. Current project considered HIL testing of one individual inverter due to equipment availability. But a full comparison with the Simulink results would need the use of multiple inverters connected to the grid emulator. More powerful real-time digital simulation platforms will be required that can interface multiple devices and cover a larger network model.
- Employ a Power Hardware-in-the-Loop (PHIL) testing, possibly including a PV panel on the dc side of the power converter. This would necessitate use of power amplifiers to interface the grid emulator to the inverter in order to allow power flow through the inverter.

The simulations followed by HIL testing have shown that the developed algorithm can provide a reduction of harmonic distortion in the network. It is highly recommended to work closely with PV farm developers to gather more data on the PV farms, and specifically the collector system and the inverter physical configuration and output filters. This will allow testing the algorithm on models that are closer to the real-time operating conditions.

The various stages of the project have shown that there are many areas where issues are likely to crop up. Therefore, it is recommended that further verification tests (such as with multiple inverters) are performed such that the algorithm is subjected to more realistic network conditions (use of actual instantaneous timeframe instead of condensed time). Following this, the algorithm can be tested in the field by employing limited number of inverters initially during low irradiation period followed by full day testing.

# 7. References


1. Atheer Habash & Grazia Todeschini, “Harmonic Mitigation Work Package One – Model Development” Report, Issue 1.0, 24 July 2020, Western Power Distribution Innovation.
2. Atheer Habash & Grazia Todeschini, “Harmonic Mitigation Work Package Two - Algorithm design, development and implementation for single inverter control” Report, Issue 1.0, 17 November 2020, Western Power Distribution Innovation.
3. Atheer Habash & Grazia Todeschini, “Harmonic Mitigation Work Package Three - Algorithm design, development and implementation for multiple inverters” Report, Issue 1.0, 21 June 2021, Western Power Distribution Innovation.
4. Atheer Habash & Grazia Todeschini, “Harmonic Mitigation Work Package Four – Hardware-in-the-Loop (HIL) Testing” Report, Issue 1.0, 02/02/2022, Western Power Distribution Innovation.
5. Engineering Recommendation G5/5, “Harmonic voltage distortion and the connection of harmonic sources and/or resonant plant to transmission systems and distribution networks in the United Kingdom” ENA, London, 2020
6. CIGRE Technical Brochure 766, “Network Modelling for Harmonic Studies”, CIGRE Joint Working Group C4/B4.38, Paris, April 2019, ISBN:978-2-85873-468-9